



Review

MEMS-based micropumps in drug delivery and biomedical applications

A. Nisar*, Nitin Afzulpurkar, Banchong Mahaisavariya, Adisorn Tuantranont

*Industrial Systems Engineering, School of Engineering and Technology (SET),
Asian Institute of Technology (AIT), P.O. Box 4, Klong Luang, Pathumthani 12120, Thailand*

Received 21 July 2007; accepted 31 October 2007

Available online 20 December 2007

Abstract

This paper briefly overviews progress on the development of MEMS-based micropumps and their applications in drug delivery and other biomedical applications such as micrototal analysis systems (μ TAS) or lab-on-a-chip and point of care testing systems (POCT). The focus of the review is to present key features of micropumps such as actuation methods, working principles, construction, fabrication methods, performance parameters and their medical applications. Micropumps have been categorized as mechanical or non-mechanical based on the method by which actuation energy is obtained to drive fluid flow. The survey attempts to provide a comprehensive reference for researchers working on design and development of MEMS-based micropumps and a source for those outside the field who wish to select the best available micropump for a specific drug delivery or biomedical application. Micropumps for transdermal insulin delivery, artificial sphincter prosthesis, antithrombogenic micropumps for blood transportation, micropump for injection of glucose for diabetes patients and administration of neurotransmitters to neurons and micropumps for chemical and biological sensing have been reported. Various performance parameters such as flow rate, pressure generated and size of the micropump have been compared to facilitate selection of appropriate micropump for a particular application. Electrowetting, electrochemical and ion conductive polymer film (ICPF) actuator micropumps appear to be the most promising ones which provide adequate flow rates at very low applied voltage. Electroosmotic micropumps consume high voltages but exhibit high pressures and are intended for applications where compactness in terms of small size is required along with high-pressure generation. Bimetallic and electrostatic micropumps are smaller in size but exhibit high self-pumping frequency and further research on their design could improve their performance. Micropumps based on piezoelectric actuation require relatively high-applied voltage but exhibit high flow rates and have grown to be the dominant type of micropumps in drug delivery systems and other biomedical applications. Although a lot of progress has been made in micropump research and performance of micropumps has been continuously increasing, there is still a need to incorporate various categories of micropumps in practical drug delivery and biomedical devices and this will continue to provide a substantial stimulus for micropump research and development in future.

© 2007 Elsevier B.V. All rights reserved.

Keywords: MEMS; Microfluidics; Micropump; Drug delivery; Micrototal analysis systems (μ TAS); Point of care testing (POCT); Insulin delivery; Artificial sphincter prosthesis; Antithrombogenic micropump; Ion conductive polymer film (ICPF); Electrochemical; Evaporation type micropump

Contents

1. Introduction	918
2. Micropumps classification	920
3. Basic micropump output parameters	921
4. Mechanical micropumps	921
4.1. Electrostatic	921
4.2. Piezoelectric	924
4.3. Thermopneumatic	925
4.4. Shape memory alloy	927
4.5. Bimetallic	927

* Corresponding author.

E-mail address: st104180@ait.ac.th (A. Nisar).

4.6.	Ion conductive polymer film	928
4.7.	Electromagnetic	929
4.8.	Phase change type	930
5.	Non-mechanical micropumps	930
5.1.	Magneto hydrodynamic	930
5.2.	Electrohydrodynamic	932
5.3.	Electroosmotic	933
5.4.	Electrowetting	934
5.5.	Bubble type	934
5.6.	Flexural planar wave (FPW) micropumps	935
5.7.	Electrochemical	935
5.8.	Evaporation type	936
6.	Discussion	937
7.	Conclusion	939
	Acknowledgements	939
	References	939

1. Introduction

Microelectromechanical systems (MEMS) is a rapidly growing field which enables the manufacture of small devices using microfabrication techniques similar to the ones that are used to create integrated circuits. In the last two decades, MEMS technologies have been applied to the needs of biomedical industry giving rise to a new emerging field called Microfluidics. Microfluidics deals with design and development of miniature devices which can sense, pump, mix, monitor and control small volumes of fluids. The development of microfluidic systems has rapidly expanded to a wide variety of fields. Principal applications of microfluidic systems are for chemical analysis, biological and chemical sensing, drug delivery, molecular separation such as DNA analysis, amplification, sequencing or synthesis of nucleic acids and for environmental monitoring. Microfluidics is also an essential part of precision control systems for automotive, aerospace and machine tool industries.

The use of MEMS for biological purposes (BioMEMS) has attracted the attention of many researchers. There is a growing trend to fabricate micro drug delivery systems with newly well developed MEMS fabrication technologies and are increasingly being applied in medical fields. MEMS-based microfluidic drug delivery devices in general include microneedles based transdermal devices, osmosis based devices, micropump based devices, microreservoir based devices and biodegradable MEMS devices.

An integrated drug delivery system (DDS) consists of drug reservoir, micropumps, valves, microsensors, microchannels and necessary related circuits. A simplified block diagram of a drug delivery system is shown in Fig. 1. A typical micropump is a MEMS device, which provides the actuation source to transfer the fluid (drug) from the drug reservoir to the body (tissue or blood vessel) with precision, accuracy and reliability. Micropumps are therefore an essential component in the drug delivery systems.

Conventional drug delivery methods such as oral medications, inhalers and subcutaneous injections do not deliver all drugs accurately and efficiently within their desired therapeutic

range. Generally most of the drugs are effective if delivered within a specific range of concentration between the maximum and minimum desired levels. Above the maximum range, they are toxic and below that range, they have no therapeutic benefit [1]. In conventional drug delivery methods such as oral delivery, etc., there is a sharp initial increase in drug concentration, followed by a fast decrease to a level below the therapeutic range [2,3]. With controlled drug delivery systems as shown in Fig. 1, appropriate and effective amount of drug can be precisely calculated by the controller and released at appropriate time by the microactuator mechanism such as micropump. The benefits of controlled drug release include site-specific drug delivery, reduced side effects and increased therapeutic effectiveness.

Micropumps are also an essential component in fluid transport systems such a micrototal analysis systems (μ TAS), point of care testing (POCT) systems or lab-on-a-chip. Micropumps are used as a part of an integrated lab-on-a-chip consisting of microreservoirs, microchannels, micro filters and detectors for precise movement of chemical and biological fluids on a micro scale. Point of care testing (POCT) system is a μ TAS to conduct diagnostic testing on site close to patients to provide better health care and quality of life. In such diagnostic systems, MEMS micropumps are integrated with biosensors on a single chip.

Reviews on research and recent methods of using BioMEMS for medicine and biological applications have been previously

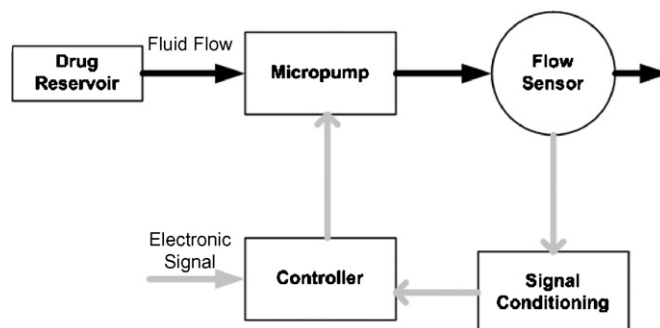


Fig. 1. Schematic illustration of drug delivery system.

published [4–7]. These reviews have reported introductory overviews on applications of BioMEMS in biomedical engineering such as surgical microsystems, therapeutic microsystems and drug therapy including devices based on microporous silicon, microneedles, micropumps, and microreservoirs, etc. Reviews on micropumps alone have also been published previously [8–10]. The last most comprehensive and excellent review on micropumps was published by Laser and Santiago [8]. However some of the novel actuation methods such as the use of polymer MEMS actuators like ion conductive polymer film (ICPF) and development of evaporation type micropumps were

not covered in the review [8]. In addition, some of the most recent and promising practical applications of micropumps in drug delivery and biomedical systems were not mentioned. The review by Woias [9] was a brief overview of a variety of micropumps and their applications. However ion conductive polymer film (ICPF), electrowetting and evaporation type micropumps were not covered in the review. The review by Tsai and Sue [10] mentioned about the technological importance of micropumps in their medical application such as drug delivery. Although this fact was mentioned in the introduction section of the review, the application of different kinds of micropumps in drug delivery

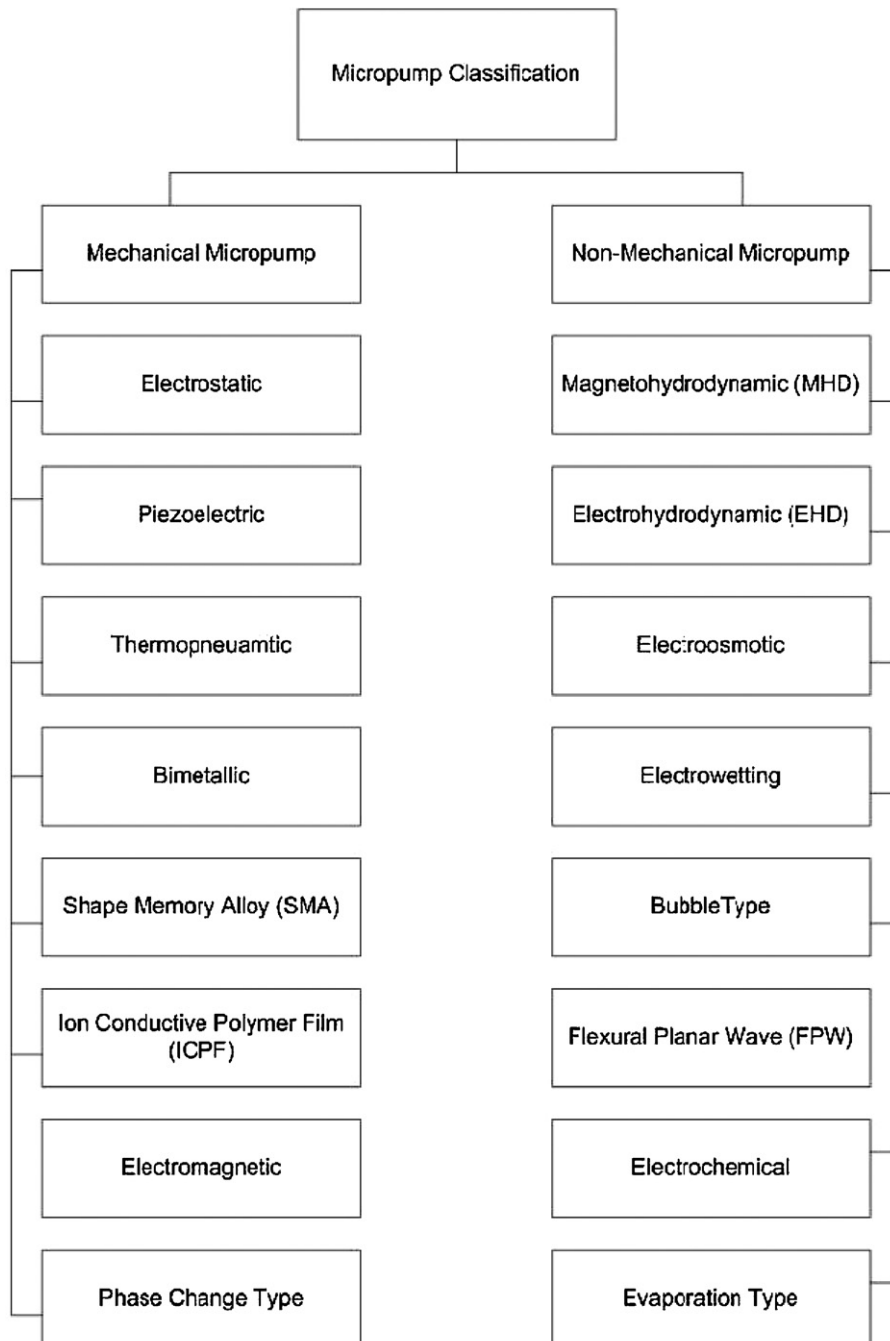


Fig. 2. Classification of micropumps with different actuation methods.

was not linked and neither mentioned in conclusions to get a global appreciation and overview of MEMS-based micropumps and their medical applications.

This review presents in depth focus on some of the novel uses of BioMEMS based various categories of micropumps and their potential applications in drug delivery and other biomedical systems such as micrototal analysis systems (μ TAS) or lab-on-a-chip. The emphasis of the review will be to present key features of micropumps such as actuation methods, working principles, construction, fabrication methods, performance parameters and their medical applications where reported.

2. Micropumps classification

According to the definition of “MEMS”, miniaturized pumping devices fabricated by micromachining technologies are called *micropumps*. In general, micropumps can be classified as either mechanical or non-mechanical micropumps [11]. The micropumps that have moving mechanical parts such as pumping diaphragm and check valves are referred to as mechanical micropumps whereas those involving no mechanical moving parts are referred to as non-mechanical micropumps.

Mechanical type micropump needs a physical actuator or mechanism to perform pumping function. The most popular mechanical micropumps discussed here include electrostatic, piezoelectric, thermopneumatic, shape memory alloy (SMA), bimetallic, ionic conductive polymer film (ICPF), electromagnetic and phase change type.

Non-mechanical type of micropump has to transform certain available non-mechanical energy into kinetic momentum so that the fluid in microchannels can be driven. Non-mechanical micropumps include magnetohydrodynamic (MHD), electrohydrodynamic (EHD), electroosmotic, electrowetting, bubble type, flexural planar wave (FPW), electrochemical and evaporation based micropump. The classification of micropumps is shown in Fig. 2.

One of the very first documents about a miniaturized micropump is a patent by Thomas and Bessman [12] which dates back to 1975. The device was designed for implantation into the human body and comprised of a solenoid valve connected to a variable pumping chamber which was actuated by two opposed piezoelectric disc benders. The device was fabricated using conventional techniques and it was not until 1984 that a micropump based on silicon microfabrication technologies was patented by Smits [13]. Smits published his results later in 1990 [14]. The micropump designed by Smits [13] was a peristaltic pump consisting of three active valves actuated by piezoelectric discs. The device was primarily developed for use in controlled insulin delivery systems.

The most common types of mechanical micropumps are displacement pumps involving a pump chamber which is closed with a flexible diaphragm. A schematic illustration of diaphragm type mechanical micropump is shown in Fig. 3. Fluid flow is achieved by the oscillatory movement of the actuator diaphragm which creates under and over pressure (Δp) in the pump chamber. Under pressure in the pump chamber results in the flow of fluid inside the pump

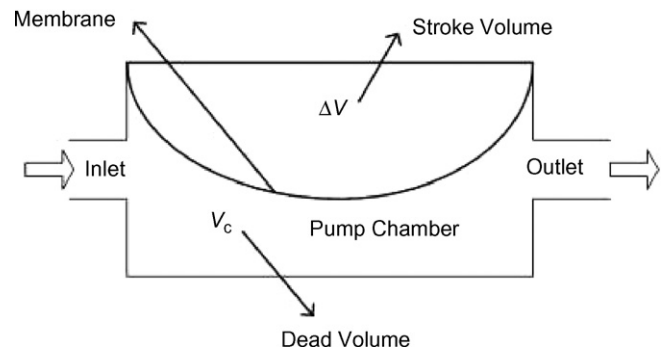


Fig. 3. Schematic illustration of diaphragm type micropump.

chamber through the inlet valve. Over pressure in the pump chamber transfers the fluid out of the pump chamber through the outlet valve. The pressure generated inside the pump chamber is a function of stroke volume (ΔV) produced by the actuator. The actuator has to contend with the dead volume (V_0) present in the pump chamber. The major design parameter of mechanical diaphragm type micropumps is called the compression ratio (ε) which is expressed as follows:

$$\varepsilon = \frac{\Delta V}{V_0} \quad (1)$$

Mechanical micropump designs may contain single pump chamber or sequentially arranged multiple pump chambers in series or in parallel. Such type of micropumps are called peristaltic micropumps. Peristaltic movement of diaphragms in the sequentially arranged pump chambers, transfers the fluid from the inlet to the outlet. A schematic illustration of peristaltic micropump based on thermopneumatic actuation is shown in Fig. 4.

Microvalves are another important element of mechanical micropumps. Microvalves are classified as passive or active valves. Passive valves do not include any actuation. The valving effect of passive valves is obtained from a difference in pressure between the inlet and the outlet of the valve. Mechanical micropumps reported in [15,16,52] have passive valves. Active valves are operated by actuating force and offer improved performance but increase complexity and fabrication cost. Active valves with electrostatic [17], thermopneumatic [18] and piezoelectric [19] actuation have been reported.

Valveless micropumps are similar to diaphragm type mechanical micropumps but do not use check valves to rectify flow. Instead nozzle/diffuser elements are used as flow rectifiers. A schematic illustration of valveless micropump is shown in Fig. 5.

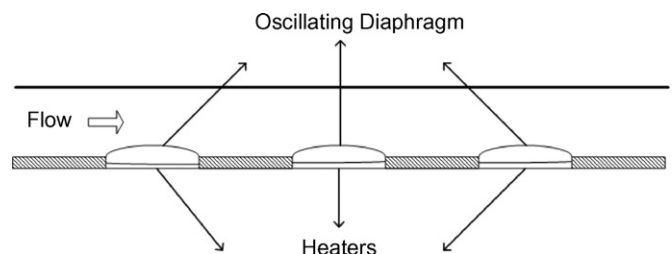


Fig. 4. Schematic illustration of peristaltic micropump.

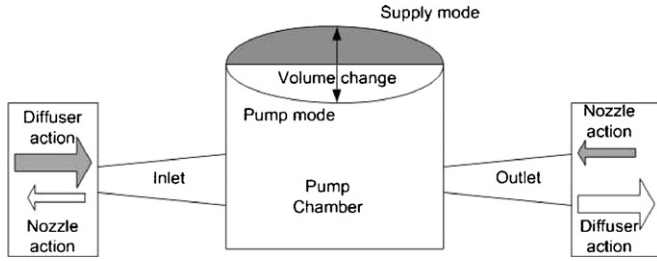


Fig. 5. Schematic illustration of valveless micropump.

The nozzle/diffuse elements direct flow such that during the supply mode, more fluid enters through the inlet than exits at the outlet. The reverse occurs for the pump mode. The first valveless miniature micropump using nozzle/diffuser as flow rectifying elements was presented in 1993 by Stemme and Stemme [20].

Micropumps for drug delivery applications must meet basic requirements, which are [21]: drug biocompatibility, actuation safety, desired and controllable flow rate, small chip size and less power consumption. Biocompatibility of MEMS-based micropumps is becoming increasingly important and is regarded as a key requirement for drug delivery systems. Biocompatibility is defined as “the ability of a material to perform with an appropriate host response in a specific application” [22]. As micropumps in drug delivery systems can be implanted inside the human body, therefore the materials used for fabrication must be able to fulfil rigorous biocompatibility and biostability requirements [23]. The implanted micropump based drug delivery system must be able to withstand long term exposure to physiological environment and resist the adverse impact of surrounding tissues on its working [24]. Therefore, biocompatibility of the materials used to fabricate MEMS-based micropumps and drug delivery system is an important materials selection parameter.

Silicon based MEMS technology has been successfully applied in biomedical field with the recent growth of implantable drug delivery systems. Silicon as substrate material has been used extensively as a good biocompatible material, however a trend towards the use of polymers as substrate material is growing as polymer materials are widely used in medicine and are suitable for human implantation. Polymer materials such as polymethylmethacrylate (PMMA), polydimethylsiloxane (PDMS), SU-8 photo resist, etc., possess relatively better biocompatibility and are increasingly being used in fabrication of MEMS micropumps.

3. Basic micropump output parameters

At the design stage, several design parameters need to be considered to optimize the micropump performance. These include maximum flow rate (\dot{Q}_{\max}), maximum back pressure (h_{\max}), pump power (P_{pump}) and pump efficiency (η). The maximum flow rate is obtained when the pump is working at zero back pressure. At the maximum back pressure, the flow rate of the pump becomes zero because back pressure opposes the work done by the pump. Pump head (h), or net head, can be derived from the steady flow energy equation assuming incompressible flow and neglecting viscous work and heat transfer. It is the work done on

a unit weight of liquid passing from the inlet to the outlet [25]:

$$h = \left(\frac{P}{\gamma} + \frac{u^2}{2g} + z \right)_{\text{out}} - \left(\frac{P}{\gamma} + \frac{u^2}{2g} + z \right)_{\text{in}} \quad (2)$$

where P is the pressure, $\gamma (= \rho g)$ the pressure head, g the acceleration of gravity, ρ the fluid density, u the fluid velocity, $u^2/2g$ the velocity head and z is the elevation.

This represents an increase in Bernoulli head from the inlet to the outlet. Usually, u_{out} and u_{in} are about the same and $z_{\text{out}} - z_{\text{in}}$ is negligible, so the maximum pump head becomes:

$$h_{\max} \approx \frac{P_{\text{out}} - P_{\text{in}}}{\gamma} = \frac{\Delta P}{\gamma} \quad (3)$$

Power delivered to the fluid by the pump is the product of the specific weight, discharge, and net head change. It can be expressed as [26]:

$$P_{\text{pump}} = p_{\max} \dot{Q}_{\max} = \rho g \dot{Q}_{\max} h_{\max} \quad (4)$$

If the power required to drive the pump actuator is P_{actuator} , pump efficiency is expressed as

$$\eta = \frac{P_{\text{pump}}}{P_{\text{actuator}}} \quad (5)$$

In an ideal pump, P_{pump} and P_{actuator} is identical as no losses exist. Efficiency is governed by fluid leakage losses (volumetric efficiency), frictional losses (mechanical efficiency), and losses due to imperfect pump construction (hydraulic efficiency). Therefore, total efficiency consists of three parts [25]:

$$\eta \equiv \eta_v \eta_m \eta_h \quad (6)$$

where η_v is the volumetric efficiency, η_m the mechanical efficiency and η_h is the hydraulic efficiency.

4. Mechanical micropumps

Mechanical micropumps based on different actuation schemes along with their construction, fabrication details and applications are discussed. Key features and performance characteristics of mechanical micropumps are summarized and referenced in Table 1.

4.1. Electrostatic

Electrostatic actuation is based on the Coulomb attraction force between oppositely charged plates. By using the parallel plate approximation to Coulomb's law, the force generated between the plates when a voltage is applied can be expressed as

$$F = \frac{dW}{dx} = \frac{1}{2} \frac{\epsilon_0 \epsilon_r A V^2}{x^2} \quad (7)$$

where F is the electrostatic actuation force, W the energy stored, ϵ ($= \epsilon_0 \epsilon_r$) the dielectric constant, A the electrode area, V the voltage applied and x is the electrode spacing.

In electrostatic micropump, the membrane of the electrostatic micropump [27–30] is forced to deflect in either direction as

Table 1
Mechanical displacement micropumps

Actuation mechanism	Reference	Structure	Size (mm)	Valves	Pump chambers	Membrane material	Voltage (V)	Frequency (Hz)	Pressure (kPa)	Flow rate ($\mu\text{L}/\text{min}$)	Pumping medium	Application reported in reference
Electrostatic	Judy et al. [27]	Polysilicon	n/r	Active	1	Polysilicon	50	n/r	n/r	n/r	n/r	Drug delivery
	Zengerle et al. [28]	Si	98 mm ³	Cantilever type	1	Silicon	170	25	2.5	70	Water	n/r
	Zengerle et al. [29]	Si–Si	98 mm ³	passive Cantilever type	1	Silicon	200	300	29	160	Water	Chemical analysis system
	Cabuz et al. [30]	Injection mold plastic	n/r	Passive	1	Metallized Kapton	160	30	20	30	Gas	Chemical and biological sensing
	Machauf et al. [33]	Si–Si	5 mm \times 5 mm	Passive	1	Electroplated nickel	50	1830	n/r	1	Water	n/r
Piezoelectric	Van Lintel et al. [34]	Glass-Si-glass	4100 mm ³	Passive	1	Glass	125	0.1	24	0.6	Water	n/r
	Stemme and Stemme [20]	Brass	2500 mm ³	Nozzle/diffuser	1	Brass	20	110	21	4400	Water	n/r
	Koch et al. [35]	Si–Si	n/r	Passive	1	Silicon	600	200	1.8	0.12	Ethanol	Drug delivery such as insulin
	Schabmueller et al. [36]	Si–Si	122.4 mm ³	Nozzle/diffuser	1	Silicon	190	2400	1	1500	Ethanol	n/r
	Junwu et al. [37]	PMMA	n/r	Cantilever type	1	Beryllium bronze	50	800	23	3500	Water	Drug delivery
	Feng and Kim [39]	Si–Si	160	Passive	1	Silicon	80	60K	0.12	3.2	Water	Implantable micropump
	Geipel et al. [40]	Si–Si	n/r	Active	1	Silicon	100	<1	10	4.5	Water	Drug delivery system for metronomic therapy or chronotherapy
	Ma et al. [41]	Si–Si	2240 mm ³	Passive	1	Silicon	67.2	208	3.43	1800	Fluid with glucose	Transdermal insulin delivery
	Doll et al. [42]	Si–Si	330 mm ³	Active	1	Silicon	n/r	27.8	60	1800	Water	Medical implant; Sphincter prosthesis
	Hsu et al. [45]	Si-glass	24 mm \times 75 mm	Passive	3	Glass	140	450	1.8	50.2	Blood	Drug delivery/ Point of Care testing(POCT)
	Suzuki et al. [46]	PDMS-glass	n/r	n/a	1	PDMS	100	87	2.4k	336	n/r	Point of Care Testing (POCT)
Thermopneumatic	Van De Pol et al. [52]	Glass-Si–Si	3000 mm ³	Flap	1	Silicon	6	1	5	34	Water	n/r
	Jeong and Yang [49]	Glass-Si-glass	n/r	Nozzle/diffuser	1	Silicon	8	4	0	14	Water	n/r
	Zimmermann et al. [50]	Glass-Si	n/r	Flap	1	n/a	n/r	10	16	9	Isopropyl alcohol	Cryogenic systems/ Drug Delivery
Thermopneumatic	Hwang et al. [54]	Glass-SU8-Si	105.3 mm ³	Capillary stop valve	1	SU-8-2100	20	n/r	n/r	3.3	Water	Drug delivery systems.
	Kim et al. [55]	PDMS-glass	n/r	Valveless (nozzle/diffuser)	1	PDMS	55	6	n/r	0.078	Methanol	Disposable Lab-on-a-chip
	Jeong et al. [56]	PDMS	n/r	Actuator as valve	3	PDMS	20	2	0	21.6	Water	Drug delivery systems
Shape memory alloy	Benard et al. [57]	Si–Si	n/r	Passive valves	1	TiNi alloy	6	0.9	4.23	49	Water	n/r
	Benard et al. [58]	Si–Si	n/r	Passive valves	1	Polyimide	n/r	0.9	0.53	6	Water	n/r
	Xu et al. [59]	Si–Si	54 mm ³	Passive valves	1	NiTi/Si	n/r	40–60	100 kPa	340	Water	n/r
	Shuxiang et al. [60]	Acryl-silicon rubber	16 mm dia. \times 74 mm length	Diffusers	1	NiTi coil actuator	6	n/r	n/a	700	Saline	Intracavity intervention
Bimetallic	Zhan et al. [61]	Si–Si	36 mm ³	n/r	1	Aluminum-Si	5.5	0.5	12	45	n/r	n/r
	Zou et al. [63]	Si-glass	182	Check valves	1	Aluminum-Si		0.5	0.5	336	Water	n/r
ICPF	Guo et al. [71]	Acryl	13 mm dia. \times 23 mm length	Active valves	2	ICPF	1.5	2.2	n/r	37.8	n/r	Biomedical
Electromagnetic	Bohm et al. [74]	Plastic	800	n/r	n/r	Plastic	5	50	0	2100	Water	n/r
	Yamahata et al. [76]	PMMA	n/r	Nozzle/diffuser	1	PDMS	n/r	12	0.02	400	Water	Lab-on-a-chip systems
	Yamahata et al. [77]	PMMA	4752 mm ³	Check valves	1	n/a	n/r	n/r	2.5	30	Water	
	Pan et al. [78]	PDMS	600mm ³	Ball check valves	1	PDMS	n/r	n/r	3.6	1000	Water	Lab-on-a-chip systems
Phase change	Sim et al. [79]		72.25 mm ³	Passive valves	1	silicon	10	0.5	0	6.1	Water	Lab-on-a-chip systems
	Boden et al. [80]	Epoxy	750 mm ³	Active valves	1	Epoxy	2	n/r	n/r	0.074	n/r	n/r

n/r: not reported.

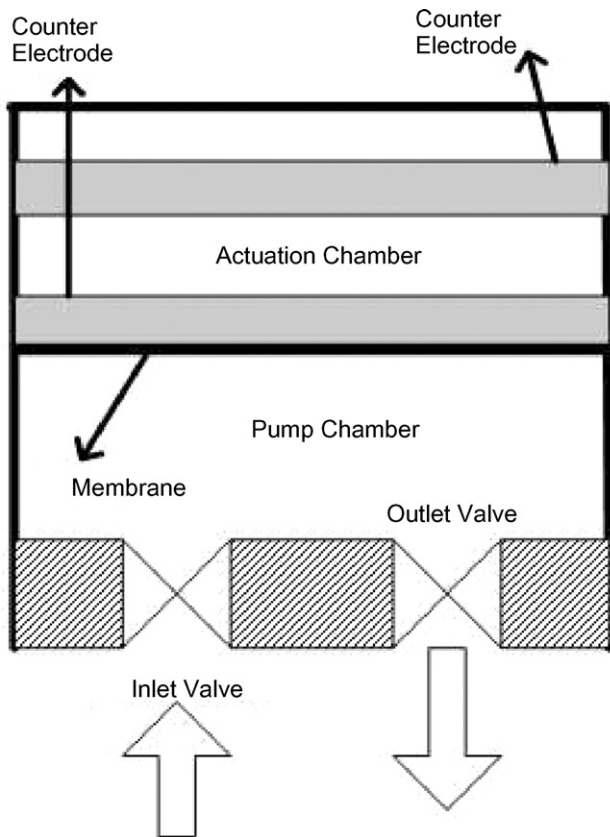


Fig. 6. Schematic illustration of electrostatic micropump.

appropriate voltage is applied on the two opposite electrostatic plates located on both sides as shown in a schematic illustration in Fig. 6. The deflected membrane is returned to its initial position if the applied voltage is cut off. The chamber volume inside the micropump varies by alternate switching of applied voltage. The fluid in reservoir is forced to flow in the microchannels due to pressure difference induced by the membrane deflection in the pump chamber. The advantages of electrostatic micropumps are low power consumption which is of the order of 1 mW and fast response time. The deflection of the diaphragm can be easily controlled by applied voltage. A major disadvantage is the small actuator stroke, which is usually limited up to $5\ \mu\text{m}$ with applied actuation voltages of around 200 V.

The first micropump based on electrostatic actuation was developed by Judy et al. [27]. It was also the first surface micromachined micropump as compared to previous bulk surface micromachined micropumps. No bulk silicon agents or wafer bonding techniques were used in its fabrication. Instead, selective deposition and etching of sacrificial layers were used to fabricate the structure. The micropump consisted of an active check valve, a pumping membrane and an active outlet valve. All parts were encapsulated by silicon nitride and were actuated by electrostatic force. Actuation voltages of approximately 50 V were required for valve closure and membrane deflection. However no pumping action was reported.

Zengerle et al. [28] developed the first working electrostatic micropump. The micropump consisted of a membrane made of four silicon layers which formed two cantilever passive valves,

pump membrane and counter electrode for electrostatic actuation. The membrane had an area of $4\ \text{mm} \times 4\ \text{mm}$ and a thickness of $25\ \mu\text{m}$. The volumetric stroke of the membrane was between 0.01 and $0.05\ \mu\text{l}$. The separation between the movable membrane and the electrically isolated stator was $4\ \mu\text{m}$. The passive valves were cantilevers measuring $1\ \text{mm} \times 1\ \text{mm}$ with thickness varying between 10 and $20\ \mu\text{m}$. During fabrication all chips were made by anisotropic etching from single side polished silicon wafers. For fabricating valves, lithography was done on front side of the wafer for flaps and orifices. Pumping was achieved for the first time at actuation frequencies in the range of 1–100 Hz. At frequency of 25 Hz and 170 V, a flow rate of $70\ \mu\text{l}/\text{min}$ at zero back pressure was achieved. In addition a maximum pressure head of 2.5 kPa was developed.

Zengerle et al. [29] later reported the development of bidirectional silicon micropump with electrostatically actuated membrane and two passive check valves. The micropump had dimensions of $7\ \text{mm} \times 7\ \text{mm} \times 2\ \text{mm}$ and contained a stack of four layers, pump membrane, passive check valves, inlet and outlet. The bidirectional pumping was dependent on actuation frequencies. At low actuation frequencies between 0.1 and 800 Hz, the micropump operated in the forward mode. At higher actuation frequencies between 2 and 6 kHz, the micropump operated in the reverse direction. The bidirectional phenomenon was due to a phase shift between the response of the check valves and a pressure difference that resulted in fluid flow. The maximum pressure achieved by the micropump was 31 kPa. The maximum volumetric flow rate was $850\ \mu\text{l}/\text{min}$ at a supply voltage of 200 V.

A dual diaphragm micropump was introduced by Cabuz et al. [30]. The micropump consisted of two diaphragms with several through holes in pump chamber. The pump chamber was made by injection molding. Electrodes were deposited by evaporation. Thin dielectric material was deposited by ion beam sputtering. The micropump was mechanically assembled. The micropump achieved flow rates of $30\ \mu\text{l}/\text{min}$ at frequency of 30 Hz and power consumption of 8 mW. The operating voltage was 160 V. The micropump operated in bidirectional mode but was applicable for gases only. This type of micropump was an ideal candidate in chemical and biological sensing applications.

The design and simulation of an electrostatic peristaltic micropump for drug delivery applications was reported by Teymoori and Sani [31]. The size of the micropump was $7\ \text{mm} \times 4\ \text{mm} \times 1\ \text{mm}$. The proposed fabrication process consisted of a silicon substrate on which membrane part was constructed and glass substrate which contained input and output ports. The simulated result for the threshold voltage of the micropump was 18.5 V. The flow rate of the designed micropump was $9.1\ \mu\text{l}/\text{min}$ which was quite suitable for drug delivery applications such as chemotherapy. The micropump was designed to satisfy major drug delivery requirements such as drug compatibility, flow rate controllability and low power consumption and small chip size. However the actual fabrication and testing of the designed micropump to verify performance parameters was not reported.

Bourouina et al. [32] reported on the design and simulation of a low voltage electrostatic micropump for drug delivery applications. The total size of the micropump was $5\ \text{mm} \times 5\ \text{mm}$. The

micropump parameters such as microchannel dimensions were chosen for drug delivery applications where a very small flow rate was involved. The working voltage was 10 V. Simulated flow rates in the range of 0.01–0.1 $\mu\text{l}/\text{min}$ were reported which were suitable for drug delivery applications. The fabrication and testing of the device for comparison with theoretical predictions was not reported.

Machauf et al. [33] reported a first attempt to fabricate a membrane micropump which was electrostatically actuated across the working fluid. The flow rate achieved was 1 $\mu\text{l}/\text{min}$ at 50 V actuation voltage. The design was based on utilizing high electric permittivity of the working fluid as well as low conductivity. The electrostatic force acting on the membrane was proportional to the working fluid electric permittivity and higher the permittivity, the higher the force and flow rate for a given applied voltage. This concept was in contrast to the micropump design described by Zengerle et al. [28] where the voltage was applied across the air gap between electrodes above the pump chamber. The advantage of the approach adopted by Zengerle et al. [28] was that the working fluid did not come under the influence of the applied electric field and thus both conductive and non-conductive fluids could be pumped in this way. The limitation, however, was the cost and complexity of the device due to the requirement to create an air gap above the pump chamber. It was accomplished with a stack of four silicon layers. As the design described by Machauf et al. [33] involved application of electric field between the pump chamber and the working fluid, the main advantage of the design was the simplicity of construction and low fabrication cost as only two silicon wafers were used. However the micropump was limited to pump only conductive fluids. The device was fabricated in silicon and the diaphragm was made of electroplated nickel. The assembly was done using flip-chip bonding.

4.2. Piezoelectric

A piezoelectric micropump consists of a piezoelectric disk attached on a diaphragm, a pumping chamber and valves. The piezoelectric micropump is actuated by the deformation of the piezoelectric materials. Piezoelectric actuation involves the strain induced by an applied electric field on the piezoelectric crystal as shown in a schematic illustration in Fig. 7.

Typical characteristics of piezoelectric actuators include large actuation force, fast response time and simple structure. However, fabrication is complex as piezoelectric materials are not easily processed. The comparatively high actuation voltage

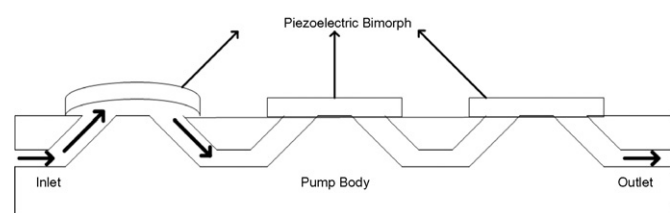


Fig. 7. Schematic illustration of piezoelectrically actuated micropump.

and small stroke, i.e. displacement per unit length are regarded as the disadvantages.

Van Lintel et al. [34] reported a first attempt to fabricate silicon micropump based on piezoelectric actuation. The reciprocating displacement type micropump was comprised of a pump chamber, a thin glass pump membrane actuated by piezoelectric disc and passive silicon check valves to direct the flow. The piezoelectric disc was attached by means of cyanoacrylate adhesive. It was the first reported work on a successfully fabricated micropump using micromachining technologies.

Koch et al. [35] proposed a typical piezoelectric micropump based on the deformation of a screen-printed piezoelectric zirconate titanate (PZT) on the silicon membrane. The micropump consisted of a stack of three silicon chips. Outlet and inlet valves were formed in the two lower layers and membrane actuator formed the top layer. The dimensions of the silicon membrane were 8 mm \times 4 mm \times 70 μm . Flow rate of up to 120 $\mu\text{l}/\text{min}$ was achieved. A maximum back pressure of 2 kPa was measured when a supply voltage of 600 V was applied at 200 Hz across a 100 μm thick piezoelectric layer. The micropump design was suitable to be applied in medicine as cheap disposable micropump for drug delivery such as insulin.

Schabmueller et al. [36] reported a piezoelectrically actuated silicon membrane micropump with passive valves. The fabrication of the micropump was based on double sided processing of silicon and bulk KOH etching. The size of the micropump was 12 mm \times 12 mm and the height including the piezoelectric zirconate titanate (PZT) disc was 0.85 mm. A flow rate of 1500 $\mu\text{l}/\text{min}$ and a back pressure of 1 kPa were achieved with ethanol as the pumping medium. In case of air as the pumping medium, a maximum flow rate of 690 $\mu\text{l}/\text{min}$ was measured.

A high performance piezoelectrically actuated cantilever valve micropump for drug delivery application was investigated by Junwu et al. [37]. The output values of the micropump were improved by the design of the cantilever valves. The micropump with shorter cantilever valves obtained higher flow rate of 3500 $\mu\text{l}/\text{min}$ and back pressure of 27 kPa. The same micropump with larger cantilever valves obtained a flow rate of 3000 $\mu\text{l}/\text{min}$ and back pressure of 9 kPa. The micropump was comprised of a structure of stacked layers which were glued together. The pump body and upper cover were made of PMMA and manufactured by conventional technology. The cantilever valves were made of precision bronze membrane. A maximum back pressure of 27 kPa achieved by the micropump was higher than the normal blood pressure of 15 kPa [38]. Therefore the micropump design was applicable for drug delivery.

Feng and Kim [39] developed a piezoelectric micropump with dome shaped diaphragm and one way parylene valves. Piezoelectric ZnO film with less than 10 μm thickness was used to actuate a parylene diaphragm fabricated on silicon substrate. The size of the micropump was 10 mm \times 10 mm \times 1.6 mm. The flow rate of 3.2 $\mu\text{l}/\text{min}$ was achieved at low power consumption of 3 mW. The operating voltage was 80 V and maximum back pressure was 0.12 kPa. The micropump was fabricated using IC compatible batch process using biocompatible materials. The low power consumption of the micropump makes it an ideal candidate for implantable micropump powered by battery.

Geipel et al. [40] reported for the first time a novel design of micropump with back flow pressure independent flow rate for low flow rate requirements such as required in drug delivery applications. The concept was based on piezoelectrically actuated diaphragms to achieve flow rates in the range of 1–50 $\mu\text{l}/\text{min}$. The major limitation which prevents volumetric dosing of a micropump is back pressure dependency. To address this undesired effect, the design reported in Ref. [40] worked on the principle of peristaltic micropump (micropump with multiple chambers in series) with no middle membrane normally used as pump membrane. Two back-to-back connected active valves controlled the fluid flow by alternate switching of three-phase actuation scheme. The fluid was drawn from the reservoir into the pump chamber until an equilibrium pressure was established. The simultaneous closing of the inlet and opening of the outlet valve moved the fluid in the desired direction. The simultaneous switching of the valves was the key characteristic of the micropump. The micropump was made from two micromachined silicon wafers in a bulk silicon process. Back pressure independency was proven up to 20 kPa for low frequencies. The back pressure independent micropump with low power consumption is ideal for application in drug delivery systems for medical treatment such as metronomic therapy or chronotherapy.

Ma et al. [41] presented the development of a novel piezoelectric zirconate titanate (PZT) insulin micropump integrated with microneedle array for transdermal drug delivery. The size of system was 8 mm \times 8 mm \times 35 mm. The microneedle array on a flexible substrate could be mounted on non-planar surface or even on flexible objects such as a human fingers and arms. The piezoelectric micropump design was based on the design published by Van Lintel et al. [34]. Flow rates were measured using different concentrations of glucose. A flow rate up to 2400 $\mu\text{l}/\text{min}$ was achieved at applied voltage of 67.2 V. The materials in contact with the drug were silicon, silicon dioxide, brass and silicon epoxy which are all biocompatible.

Doll et al. [42] presented novel medical implant based on bidirectional micropump for artificial sphincter system. The fecal incontinence is the loss of natural and sphincter control and can lead to unwanted loss of feces. There are several treatment options such as biofeedback training, strengthening of the pelvic floor and reconstructive surgical methods with autologous materials but with limited success. The German artificial sphincter system (GASS) is in fact a hydraulic muscle for treatment of fecal incontinence [43,44]. The design reported by Doll et al. [42] was an integrated structure with all functions in one device with a piezoelectrically actuated peristaltic micropump embedded in the system. The micropump was fabricated in silicon and the pump chamber and the valve lip were fabricated by silicon etching process. The micropump achieved a flow rate of 1800 $\mu\text{l}/\text{min}$ and was able to buildup and maintain backpressures up to 60 kPa. The overall size of the micropump was 30 mm \times 11 mm \times 1 mm. The micropump featured active valves which enabled the reversal of the pump direction by applying different actuation schemes.

Hsu et al. [45] investigated development of antithrombotic micropumps for blood transportation tests. A peristaltic

micropump based on piezoelectric actuation was developed to transport whole blood. The micropump performance was evaluated using deionised water and whole blood. The micropump was comprised of three parts, silicon, pyrex glass and a commercially available bulk piezoelectric zirconate titanate (PZT) material. Silicon etching process was used to fabricate pump chambers and channels. Three pieces of 12 mm square bulk piezoelectric zirconate titanate (PZT) chips with a thickness of 191 μm were glued on to the silicon membrane using silver epoxy. The total size of the micropump was 24 mm \times 75 mm. To prevent blood from clotting (thrombosis) in the micropump, two materials, polyethylene oxide urethane (PEOU) and polyethylene glycol (PEG) were used to form a monolayer on the surface of the chip. The flow rate of the micropump using deionised water was 121.6 $\mu\text{l}/\text{min}$ at 500 Hz and 140 V and maximum back pressure of 3.2 kPa. The flow rate for blood was 50.2 $\mu\text{l}/\text{min}$ at 450 Hz and 140 V and maximum back pressure of 1.8 kPa. The designed micropump reported in Ref. [45] has tremendous potential in biomedical applications such as drug delivery.

Suzuki et al. [46] proposed a travelling wave piezoelectrically actuated micropump for point of care testing (POCT) system. The system reported in Ref. [46] comprised of integrated travelling wave micropump and miniaturized surface plasmon resonance (SPR) imaging sensor on one chip. Surface plasmon resonance (SPR) imaging is one of the most suitable biosensor for μTAS . SPR biosensor is used to detect the specific biosample with real time multisensing analysis. The micropump comprised of an array of piezoelectric actuators to induce a travelling wave in a PDMS microchannel. The maximum flow rate achieved by the micropump was 336 $\mu\text{l}/\text{min}$. The SPR imaging measurements with bovine serum albumin solutions were carried out using the prototype diagnostic system.

The major limitation of the piezoelectrically actuated micropumps is the requirement of high supply voltages. In addition, the application of piezoelectric discs is not compatible with integrated fabrication. Nevertheless, mechanical micropumps based on piezoelectric actuation have grown to be the dominant type of micropumps in drug delivery systems and optimization of the geometrical design of piezoelectric micropump has been done to achieve higher strokes at lower voltages [47,48].

4.3. Thermopneumatic

In thermopneumatic micropump, the chamber which is full of air inside, is expanded and compressed periodically by a pair of heater and cooler as shown in Fig. 8. The periodic change in volume of chamber actuates the membrane with a regular movement for fluid flow.

Thermopneumatic actuation involves thermally induced volume change and/or phase change of fluids sealed in a cavity with at least one compliant wall. For liquids, the pressure increase is expressed as

$$\Delta P = E \left(\beta \Delta T - \frac{\Delta V}{V} \right) \quad (8)$$

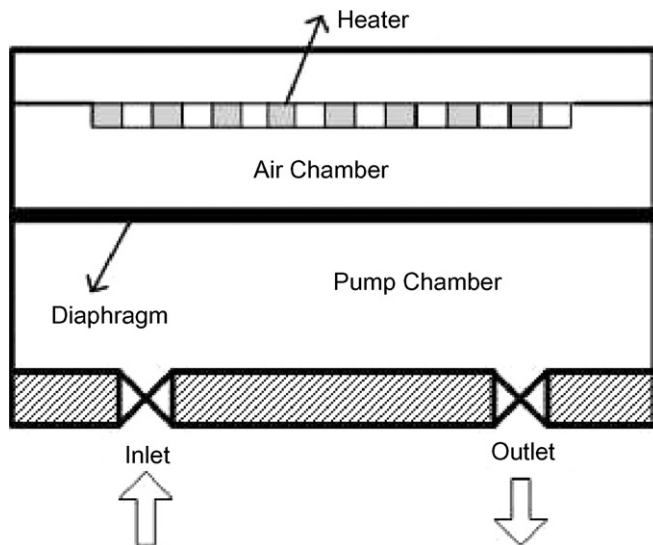


Fig. 8. Schematic illustration of thermopneumatic micropump.

where ΔP is the pressure change, E the bulk modulus of elasticity, β the thermal expansion coefficient, ΔT the temperature increase and $\Delta V/V$ is the volume change percentage.

For simplicity we assume that there is no volume expansion and for water as the fluid we take the value of $E = 3.3 \times 10^5$ psi and $\beta = 2.3 \times 10^{-4} \text{ } ^\circ\text{C}^{-1}$ in Eq. (8). Thus, for water, the temperature dependent pressure change can be expressed as 76 psi/ $^\circ\text{C}$ for the above conditions. Such a large pressure translates to large deflections and forces but suffer from high-power consumption and slow response time which are characteristic of thermal actuation methods.

The thermopneumatic type of micropumps [49–51] generate relatively large induced pressure and displacement of membrane. However, on the other hand, the driving power has to be constantly retained above a certain level. Until 1990, all micropump designs developed were based on piezoelectric bimorph or monomorph discs for actuation. In order to fabricate micropump using microengineering techniques such as thin film technology, photolithography techniques and silicon micromachining, researchers looked for micromachinable actuators. The first piece of work on the utilization of micromachinable actuators was carried out by Van De Pol et al. [52]. The thermopneumatic actuation principle was adopted from Zdelblich et al. [53] who reported the first thermopneumatic micropump. The micropump was a reciprocating displacement micropump with passive valves. The actuator comprised of a cavity filled with air, a square silicon pump membrane and built in aluminum meander, which served as a resistive heater. The application of an electric voltage to the heater caused a temperature rise of the air inside the cavity and a related pressure increase induced a downward deflection of the pump membrane causing pressure increase in the pump chamber. The pressure difference resulted in opening and closing of the inlet and outlet valves respectively. A maximum flow rate of 34 $\mu\text{l}/\text{min}$ was reported at 5 kPa pressure and 6 V.

Jeong et al. designed a thermopneumatic micropump [49] with a corrugated diaphragm. The thermopneumatic micropump

had a pair of nozzle/diffuser and an actuator with corrugated diaphragm and a microheater. The base material for actuator diaphragm was double side polished 450 μm thick n-type (1 0 0) silicon wafer. The flow rates of the micropump with the corrugated diaphragm and that with the flat one were measured. For the same input power, the maximum flow rate of the micropump with the corrugated diaphragm was 3.3 times that with the flat one. The maximum generated pressure reached 2.5 kPa. The maximum flow rate of the micropump with corrugated diaphragm reached 14 $\mu\text{l}/\text{min}$ at 4 Hz when the input voltage and duty ratio were 8 V and 40%, respectively.

Zimmermann et al. [50] developed a thermopneumatic micropump for high pressure/high flow rate applications such as cryogenic systems but worked equally well where low flow rates and precise volume control are necessary such as drug delivery systems. The micropump was planar and fabricated using a wafer-level, four-mask process. A pressure of 16 kPa and maximum flow rate of 9 $\mu\text{l}/\text{min}$ was achieved at an average power consumption of 180 mW.

Hwang et al. [54] reported a submicroliter level thermopneumatic micropump for transdermal drug delivery. The micropump comprising of two air chambers, a microchannel and stop valve, was fabricated by the spin coating process. The thermopneumatic chamber consisted of ohmic heaters on the glass substrate. The negative thick photoresist was used to form the microchannels and the two air chambers on the glass substrate. The glass plate was bonded with silicon substrate by heating. The total size of the micropump was 13 mm \times 9 mm \times 0.9 mm and the resistance of the microheater was 690 Ω . The discharge volumes were 0.1 μl for 3 s at 15 V and 0.1 μl for 1.8 s at 20 V. The designed micropump was feasible for submicroliter level drug delivery systems.

Kim et al. [55] presented a thermopneumatically actuated polydimethylsiloxane (PDMS) micropump with nozzle/diffuser elements for applications in micrototal analysis systems (μTAS) and lab-on-a-chip. The micropump consisted of a glass layer, an indium tin oxide (ITO) heater, a PDMS thermopneumatic chamber, a PDMS membrane and a PDMS cavity. The micropump was fabricated using spin coating process. The thickness of the PDMS membrane was 770 μm . A maximum flow rate of 0.078 $\mu\text{l}/\text{min}$ was observed for applied pulse voltage of 55 V at 6 Hz. The performance of the micropump is applicable for disposable lab-on-a-chip systems.

Jeong et al. [56] reported fabrication and test of a peristaltic thermopneumatically actuated PDMS micropump. The micropump consisted of microchannels, three pump chambers, inlet and outlet ports and three actuators. All parts except the microheater were fabricated with PDMS elastomer. The thermopneumatic actuators were operated as the dynamic valves and controlled easily by sequencing of three phase electric input power. Thus the design was simplified as there was no need to fabricate additional parts such as check valves. Back flow was also eliminated as the two pump chambers were always closed at a time. The diameter of the 30 μm , thick actuator diaphragm was 2.5 mm. The maximum flow rate of the micropump was 21.6 $\mu\text{l}/\text{min}$ at 2 Hz at zero pressure difference, when the three-phase input voltage was 20 V. The flow rate achieved by the micropump was

applicable to microliter level fluid control systems such as drug delivery systems.

4.4. Shape memory alloy (SMA)

Shape memory alloy (SMA) actuated micropumps make use of the shape memory effect in SMA materials such as titanium nickel. The shape memory effect involves a phase transformation between two solid phases. These two phases are called the austenite phase at high temperature and martensite phase at low temperature. In SMA materials, the martensite is much more ductile than austenite and this low temperature state can undergo significant deformation by selective migration of variant boundaries in the multi variant grain structures. When heated to the austenite start temperature, the material starts to form single variant austenite. If the material is not mechanically constrained, it will return to predeformed shape, which it retains if cooled back to the martensite phase. If the material is mechanically constrained, the material will exert a large force while assuming the pre-deformed shape. These phase transitions result in mechanical deformation that is used for actuation. High power consumption is required and the response time is slow. Shape memory alloys are special alloys such as Au/Cu, In/Ti, and Ni/Ti. A schematic illustration of SMA micropump is shown in Fig. 9.

The diaphragm of SMA micropumps [57–60] is usually made of material titanium/nickel alloy (TiNi). TiNi is an attractive material as an actuator for micropumps because its high recoverable strain and actuation forces enable large pumping rates and high operating pressures. High work output per unit volume makes it suitable in sizes for MEMS applications. The first SMA micropump was reported in 1997 by Benard et al. [57]. Two TiNi membranes were separated by a silicon spacer. Both fixed and cantilever check valves were fabricated to rectify flow. The reciprocating motion was generated by alternating the joule heating to the two TiNi membranes. Upon heating the top TiNi layer, the actuator was positioned in its most downward position.

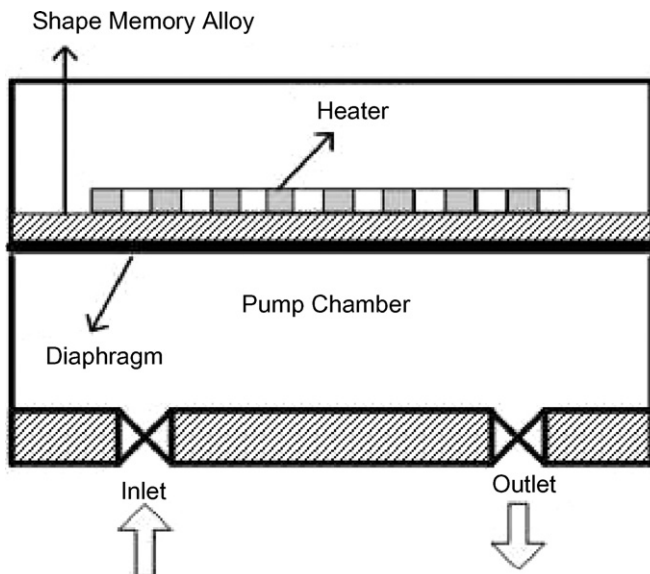


Fig. 9. Schematic illustration of shape memory alloy (SMA) micropump.

The maximum flow rate achieved was 49 $\mu\text{l}/\text{min}$ at an operating frequency of 0.9 Hz. The back pressure of 4.23 kPa was achieved. The operating current and voltage were 0.9 A and 6 V, respectively, and power consumption was 0.5 W. A polyimide spring biased SMA micropump was reported by Benard et al. [58]; however the flow rate was much lower than the flow rate reported in Ref. [57].

Xu et al. [59] reported the structure of a micro SMA pump. Its overall size was about 6 mm \times 5 mm \times 1.5 mm. The micropump was composed of a NiTi/Si composite driving membrane, a pump chamber and two inlet and outlet check valves. The volumetric flow rate and back pressure of the micropump were 340 $\mu\text{l}/\text{min}$ and 100 kPa, respectively. The micropump designs reported in Refs. [57,58] were actuated by free standing SMA thin films requiring special bias structure to get SMA effect and special structure to separate working fluid from driving circuits. This made the fabrication difficult. When utilizing a NiTi/Si composite driving membrane as reported in Ref. [59], no special bias structure was needed because silicon substrate provided the biasing force and no isolated structure was needed because silicon structure separated the working fluid from SMA film completely. SMA effect was achieved by combined action of thermal stress and substrate bias force. Thus the structure of the micropump was simplified giving a large flow rate, excellent driving efficiency and long fatigue life.

Shuxiang and Fukuda [60] developed SMA actuated micropump for biomedical applications. The micropump was comprised of SMA coil actuator as the servo actuator, two diffusers as one-way valves, a pump chamber made of elastic tube, and a casing. The SMA coil actuator utilized in this micropump was a TiNi wire with a diameter of 0.2 mm. The overall size of the micropump was 16 mm in diameter and 74 mm in length. The body of the micropump was made from acryl and chamber was made from silicon rubber. The flow rate of 500–700 $\mu\text{l}/\text{min}$ was obtained by changing the frequency. The designed micropump was able to demonstrate microflow and was suitable for the use in medical applications and in biotechnology such as intracavity intervention in medical practice for diagnosis and surgery.

4.5. Bimetallic

Bimetallic actuation is based on the difference of thermal expansion coefficients of materials. When dissimilar materials are bonded together and subjected to temperature changes, thermal stresses are induced and provide a means of actuation. Even though the forces generated may be large and the implementation can be extremely simple, the deflection of the diaphragm achieved are small because the thermal expansion coefficients of materials involved are also small. Although bimetallic micropumps require relatively low voltages compared to other types of micropumps, but are not suitable to operate at high frequencies.

A schematic illustration of bimetallic micropump is shown in Fig. 10. The diaphragm is made of two different metals that exhibit different degrees of deformation during heating [61,62]. The deflection of a diaphragm, made of bimetallic materials, is achieved by thermal alternation because the two chosen materials possess different thermal expansion coefficients.

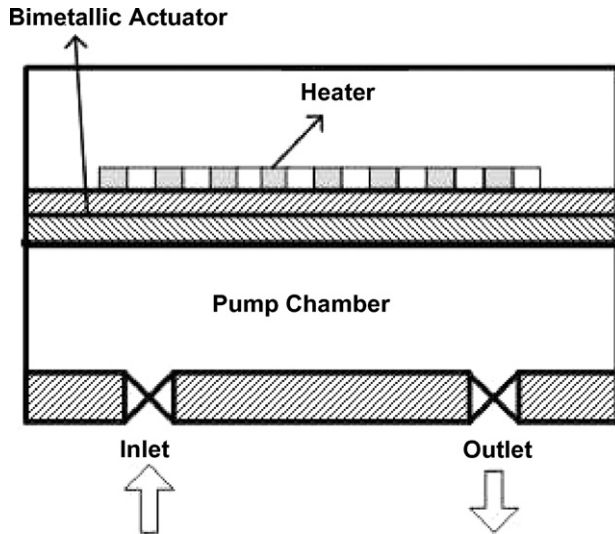


Fig. 10. Schematic illustration of bimetallic micropump.

Zhan et al. [61] designed a silicon-based bimetallic membrane, for a specific micropump. A micro-driving diaphragm was made by depositing a 10 μm thick layer of aluminum on the silicon substrate. The overall size of the micropump was about 6 mm \times 6 mm \times 1 mm. The flow rate and maximum back pressure were approximately 45 $\mu\text{l}/\text{min}$ and 12 kPa, respectively, while 5.5 V driving voltage at 0.5 Hz was applied.

Zou et al. [63] reported a novel thermally actuated micropump. This micropump utilized both bimetallic thermal actuation and thermal pneumatic actuation. The structure of the micropump was composed of two chambers (air and water), a bimetallic microactuator and two-micro check valves. The overall size of the micropump was 13 mm \times 7 mm \times 2 mm. The bimetallic actuator was made of aluminum membrane and a silicon membrane. When the bimetallic actuator was heated, the membrane was deformed downwards to press the fluid. At the same time, the gas in the air chamber was heated and expanded to strengthen the bimetallic actuation. The pressure flow characteristics of micro check valve were reported. When the open pressure of the valve was 0.5 kPa, the flow rate of the valve reached 336 $\mu\text{l}/\text{min}$.

Pang et al. [64] utilized bimetallic and electrostatic actuation for driving and controlling of the micropumps and microvalves in a single integrated microfluidic system. The microfluidic chip of the size of 5.9 mm \times 6.4 mm was comprised of micropumps, valves, channels, cavities and other different sensors. Both bimetallic and electrostatic actuation was used to actuate the micropumps and valves. On the valve membrane, two aluminum structures were designed to provide bidirectional deformation. Bimetallic driving deformation of the micropump membrane in only the up direction was designed. Bimetallic elements consisted of heating elements, top aluminum layer and bottom mechanical membrane. The dimensions of the micropump driving membrane were 1 mm \times 1 mm \times 2 μm . The size of the valve membrane was 6 mm \times 0.6 mm \times 2 μm . In the microfluidic chip, 3D structures were formed using surface and bulk micromachining followed by standard IC compatible processes to fabricate driving circuits and other sensors.

4.6. Ion conductive polymer film (ICPF)

Polymer MEMS actuators can be actuated in aqueous environment with large deflection and require less power input than conventional MEMS actuators. One of the most popular polymer actuators is ion conductive polymer film actuator (ICPF) which is actuated by stress gradient by ionic movement due to electric field. ICPF is composed of polyelectrolyte film with both sides chemically plated with platinum. Due to the application of electric field, the cations included in the two sides of the polymer molecule chain will move to the cathode. At the same time, each cation will take some water molecules to move towards the cathode. This ionic movement causes the cathode of ICPF to expand and anode to shrink. When there is an alternating voltage signal, the film bends alternately. A schematic illustration of the structure of ICPF actuator is shown in Fig. 11A. The bending principle of ICPF actuator is shown in Fig. 11B.

The ICPF actuator is commonly called artificial muscle because of its large bending displacement, low actuation voltage and biocompatibility. Researches have reported applications of ICPF in robotic [65], medical devices [66] and micromanipulators [67].

Guo et al. [68–71] reported development of ICPF polymer actuator-based micropump for biomedical applications. The

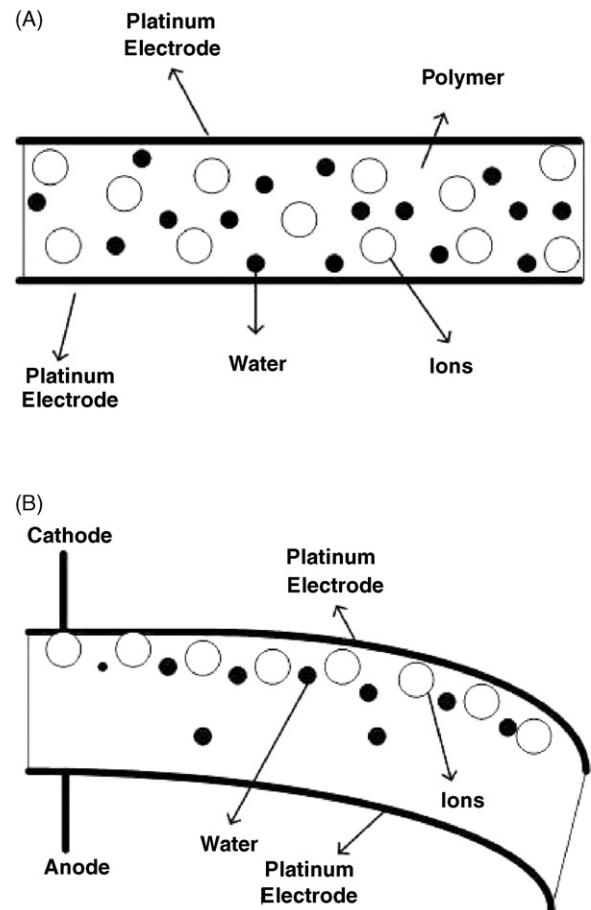


Fig. 11. (A) Schematic illustration of the structure of an ICPF and (B) schematic illustration of an ICPF bending principle.

micropump comprised of the ICPF actuator as the diaphragm, pump chamber and two one way check valves driven by ICPF actuators. ICPF actuators were installed in series to achieve high flow rates. The size of the micropump reported in Ref. [68] was 13 mm in diameter and 23 mm in length. The flow rate of the micropump was 4.5–37.8 $\mu\text{l}/\text{min}$ at 1.5 V driving voltage. The micropump design with low power consumption, biocompatibility and adequate flow rate, has potential application in medical field and biotechnology.

Guo et al. have also reported application of ICPF actuator in other areas such as artificial fish micro robot [72,73] with potential applications in medical field such as performing delicate surgical operation supported by microrobot to avoid unnecessary incisions. ICPF actuator has certain advantages such as low driving voltage, quick response, and biocompatibility. Besides, it can work in aqueous environments. The major limitation is complex fabrication of ICPF actuator.

4.7. Electromagnetic

Micromagnetic devices in general consist of soft magnetic cores and are activated by currents in energized coils or use permanent magnets. A wire carrying a current in the presence of a magnetic field will experience the Lorentz force given below:

$$F = (I \times B)L \quad (9)$$

where F is the electromagnetic (Lorentz) force, I the current passing through wire, B the magnetic field and L is the length of wire.

The force generated is large, however, electromagnetic actuation requires external magnetic field usually in the form of a permanent magnet. A schematic illustration of magnetically actuated micropump is shown in Fig. 12.

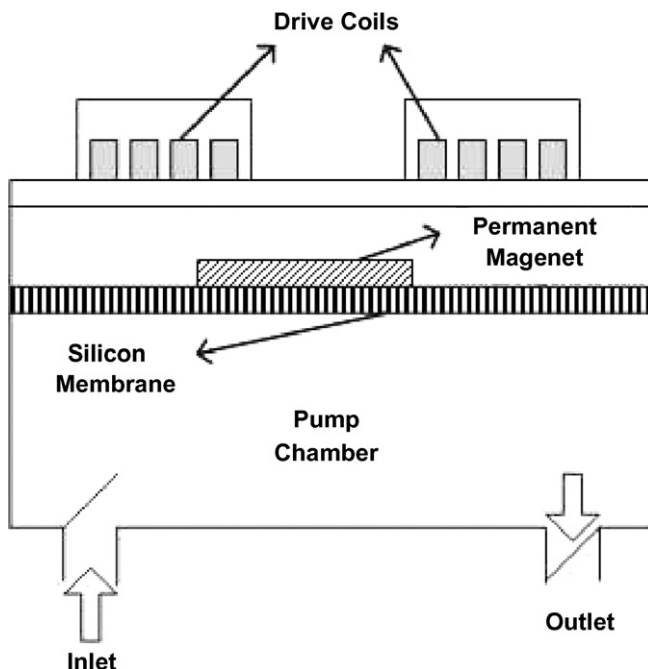


Fig. 12. Schematic illustration of a magnetically actuated micropump.

A typical magnetically actuated micropump consists of a chamber with inlet and outlet valves, a flexible membrane, a permanent magnet and a set of drive coils. Either the magnet or the set of coils may be attached to the membrane. When a current is driven through the coils, the resulting magnetic field creates an attraction or repulsion between the coils and the permanent magnet which provides the actuation force.

Electromagnetic actuation provides large actuation force over longer distance as compared to electrostatic actuation. It also requires low operating voltage. However, the electromagnetic actuation does not benefit from scaling down in size because electrostatic force reduces by the cube of scaling factor. Therefore its utilization for microfabricated actuators is limited as only a few magnetic materials can be micromachined easily. In general, electromagnetic micropumps have high power consumption and heat dissipation.

An electromagnetic actuator was proposed by Bohm et al. [74]. Plastic micropump with reasonable performance was fabricated using conventional micromechanical production methods. The micropump comprised of two folded valves parts with a thin valve membrane in between. The inlet and outlet were situated on the bottom side of the micropump, while the micropump membrane was placed on the top. An electromagnetic actuator consisting of a permanent magnet placed in a coil was used in combination with a flexible micropump membrane. Power consumption was 0.5 W and flow rates of 40,000 $\mu\text{l}/\text{min}$ for air and 2100 $\mu\text{l}/\text{min}$ for water were achieved. A relatively large volume was occupied by the electromagnetic coil, therefore the micropump final dimensions (10 mm \times 10 mm \times 8 mm) were slightly large.

Gong et al. [75] reported design optimization and simulation of a four layer electromagnetic micropump. The designed micropump consisted of electromagnetic actuator, pump chamber, passive microvalves and inlet and outlet interfaces. The micro electromagnetic actuator located on the top of the membrane, was made of planar coils. The dimensions of the actuator and the pumping membrane were 6 mm \times 6 mm and 3 mm \times 3 mm, respectively. The simulation results showed that maximum flow rate up to 70 $\mu\text{l}/\text{min}$ was achievable at a frequency of 125 Hz.

Yamahata et al. [76] described the fabrication and characterization of electromagnetically actuate polymethylmethacrylate (PMMA) valveless micropump. The complete micropump was a three-dimensional structure comprising of four sheets of PMMA fabricated by standard micromachining techniques. The micropump consisted of two diffuser elements, and a polydimethylsiloxane (PDMS) membrane with an integrated magnet made of NdFeB (neodymium, iron, and boron) magnetic powder. A large stroke membrane deflection up to 200 μm was obtained using external actuation by an external magnet. Flow rate up to 400 $\mu\text{l}/\text{min}$ and back pressure up to 1.2 kPa was measured at resonant frequencies of 12 and 200 Hz. The combination of nozzle/diffuser elements with an electromagnetically actuated PDMS membrane provided large deflection amplitude and adequate flow rates both for water and air and the concept could be successfully applied for low cost and disposable lab-on-a-chip systems.

Yamahata et al. [77] reported development of new type of micropump based on magnetic actuation of the magnetic liquid. The ferrofluid was not in direct contact with the pumping liquid. It was externally actuated by NdFeB (neodymium, iron, and boron) permanent magnet. The micropump was a three dimensional microstructure fabricated by standard micromachining techniques. The working principle was based on the oscillatory motion of the ferrofluidic liquid in a microchannel. The ferrofluid served both as an actuator and seal. The linear motion of the ferrofluid was induced by the controlled mechanical movement of the external magnet resulting in the pulsed flow by periodic opening and closing of the check valves. A flow rate of $30 \mu\text{l}/\text{min}$ was achieved at a back pressure of 2.5 kPa.

Pan et al. [78] reported on the design, fabrication and test of a magnetically actuated micropump with PDMS membrane and two one way ball check valves for lab-on-a-chip and microfluidic systems. The micropump comprised of two functional PDMS layers. One layer was used for holding ball check valves and an actuating chamber while the other layer contained a permanent magnet for actuation. The micropump could be actuated by external magnetic force provided by another magnet or internal magnetic coil. External actuation of the membrane mounted magnet provided a flow rate of $774 \mu\text{l}/\text{min}$ at power consumption of 13 mW. Alternate actuation of the micropump by a 10 turn planar microcoil fabricated on a PC board provided a flow rate of $1000 \mu\text{l}/\text{min}$. The microcoil drive was fully integrated and provided higher pumping rates at the expense of much higher power consumption.

4.8. Phase change type

The actuator in phase change type of micropumps is composed of a heater, a diaphragm and a working fluid chamber. The actuation of the diaphragm is achieved by the vaporization and condensation of the working fluid. A schematic illustration of phase change type micropump is shown in Fig. 13.

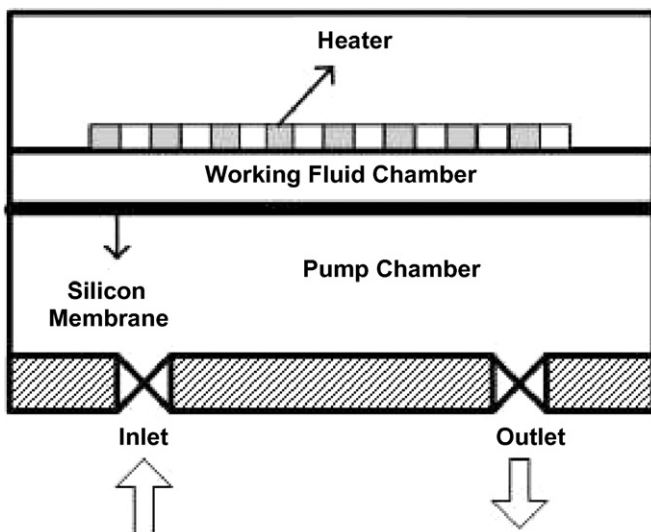


Fig. 13. Schematic illustration of a phase change type micropump.

Sim et al. [79] presented a phase change type of micropump with aluminum flap valves. The micropump consisted of a pair of passive valves and a phase change type actuator. The dimensions of the micropump were $8.5 \text{ mm} \times 5 \text{ mm} \times 1.7 \text{ mm}$. The actuator was composed of a flexible silicon membrane on a silicon substrate and a microheater on a glass substrate. When the input power was applied to the microheater, the working fluid was heated and vaporized causing pressure increase in the working fluid chamber and deflection of the membrane. When the power supply was cut off, the membrane was restored due to condensation of the working fluid. The maximum flow rate of the micropump was $6.1 \mu\text{l}/\text{min}$ at supply voltage of 10 V at 0.5 Hz. The maximum back pressure at zero flow rate was 68.9 kPa. The low flow rate of this type of micropump was suitable for application in lab-on-a-chip requiring flow rates less than few $\mu\text{l}/\text{min}$ and back pressures less than 68.9 kPa.

Boden et al. [80] reported a paraffin micropump with active valves. Identical membrane actuators activated the pump chamber and active valves. Heaters were integrated inside the paraffin. When the paraffin was melted by the heaters, the membrane sealed the inlet and outlet holes. The membrane returned to its original shape when the paraffin solidified. By a sequence of melting and solidification of the paraffin, the pumping action was achieved. A flow rate of $0.074 \mu\text{l}/\text{min}$ was achieved at an applied voltage of 2 V.

5. Non-mechanical micropumps

Non-mechanical micropumps require the conversion of non-mechanical energy to kinetic energy to supply the fluid with momentum. These phenomena are practical only in the microscale. In contrast to mechanical micropumps, non-mechanical pumps generally have neither moving parts nor valves so that geometry design and fabrication techniques of this type of pumps are relatively simpler. However they have limitations such as the use of only low conductivity fluids in electrohydrodynamic micropumps. Moreover the actuation mechanisms are such that they interfere with the pumping liquids. Since the early 1990s, many non-mechanical micropumps have been reported. Non-mechanical micropumps with different actuation methods are discussed below. Key features and performance characteristics of mechanical micropumps are summarized and referenced in Table 2.

5.1. Magnetohydrodynamic (MHD)

Magnetohydrodynamic theory is based on the interaction of the electrically conductive fluids with a magnetic field. The concept of magnetohydrodynamic (MHD) micropump is new and one of the first developed MHD micropumps was developed by Jang and Lee [81] in 1999. MHD refers to the flow of electrically conducting fluid in electric and magnetic fields. The typical structure of the MHD micropump is relatively simple with microchannels and two walls bounded by electrodes to generate the electric field while the other two walls bounded by permanent magnets of opposite polarity for generating the magnetic field. In magnetohydrodynamic micropumps, Lorentz

Table 2
Mechanical displacement micropumps

Actuation mechanism	Reference	Fabricated structure	Size (mm)	Voltage (V)	Pressure (kPa)	Flow rate ($\mu\text{l}/\text{min}$)	Pumping medium	Application reported in reference
MHD-DC type	Jang and Lee [81]	Si-Si	n/r	60	0.17	63	Seawater	n/r
	Huang et al. [82]	PMMA	n/r	15	n/r	1200	n/r	Drug delivery, biomedical studies
MHD-AC type	Heng et al. [83]	Glass-PMMA	n/r	15	n/r	1900	n/r	n/r
	Lemoff and Lee [85]	Glass-Si-glass	n/r	n/a	0	18	NaCl solution	n/r
EHD	Ritcher and Sandmaier [86]	Si-Si	3 mm \times 3 mm	600	0.43	14000	Ethanol	n/r
	Fuhr et al. [87]	Si-glass	n/r	40	n/r	2	Water	n/r
	Darabi et al. [88]	Ceramic	638.4 mm ³	250	0.78	n/r	3MHFE-7100	n/r
Electroosmotic	Zeng et al. [91]	Packed silica particles	85 mm ³	2000	2000	3.6	Water	n/r
	Chen and Santiago [92]	Soda-lime glass	9000 mm ³	1000	33	15	Water	n/r
	Takemori et al. [94]	Si-plastic	n/r	2000	10	0.1	Degassed 50 mm Trisborate buffer (pH 9.3)	n/r
	Wang et al. [95]	Fused silica-glass	n/r	6000	25	2.6	Water	Micro-analysis systems
Electrowetting Bubble type	Yun et al. [96]	Glass-SU8-Si-Si	n/r	2.3	0.7	170	Water	n/r
	Tsai and Lin [97]	Glass-Si	n/r	20	0.38	4.5	Isopropyl alcohol	n/r
	Zahn et al. [99]	SOI-quartz dice	n/r	n/r	3.9	0.12	Water	Continuous monitoring DDS/ monitor glucose levels fro diabetes patients
FPW	Luginbuhl et al. [103].	Silicon-platinum-sol-gel-derived piezoelectric ceramic	n/r	n/r	n/r	0.255	Water	n/r
	Nguyen et al. [104]	Aluminum, piezoelectric zinc oxide, silicon nitride	n/r	n/r	n/r	n/r	Water	μ TAS, cell manipulating systems, and drug delivery systems.
Electrochemical	Suzuki and Yoneyama [107]	Glass-Si	n/r	n/r	n/r	n/r	Standard solution of CuSO ₄	Drug delivery
	Yoshimi et al. [108]	Glass-platinum electrode	n/r	3	n/r	n/r	Neurotransmitter solution	Administration of neurotransmitters to neurons. Create Synapses in artificial sensory organs.
	Kabata and Suzuki [109]	Glass-platinum electrode-polyimide	n/r	1.4	n/r	13.8	Insulin	Injection of insulin and monitoring of glucose concentration
Evaporation based	Effenhauser et al. [110]	Plexiglass	n/r	n/r	n/r	0.35	Ringers solution	Continuous monitoring DDS/continuous glucose monitoring for diabetes patients

n/r: not reported.

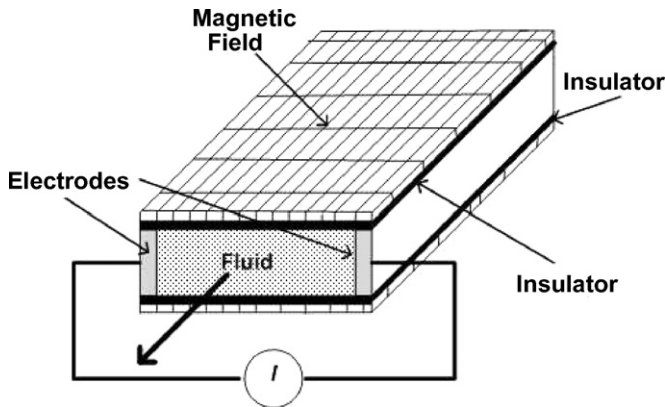


Fig. 14. Schematic illustration of MHD micropump.

force is the driving source which is perpendicular to both electric field and magnetic field [82–85]. The working fluid to be used should have a conductivity 1 s/m or higher, in addition to externally providing electric and magnetic fields. In general MHD micropumps can be used to pump fluids with higher conductivity. This greatly widens the utilization of MHD micropumps in medical biological applications. The bubbles generation due to ionization is regarded as a major drawback of MHD micropumps. A schematic illustration of MHD micropump is shown in Fig. 14.

Jang and Lee [81] investigated performance of the MHD device by varying the applied voltage from 10 to 60 V while the magnetic flux density was retained at 0.19 T. The working fluid used was seawater. The maximum flow rate reached to 63 $\mu\text{l}/\text{min}$ when driving current was retained at 1.8 mA. The maximum pressure head, 124 kPa, from inlet to outlet was obtained if the driving current was set and retained at 38 mA.

Huang et al. [82] reported design, microfabrication and test of DC type MHD micropump using LIGA microfabrication method. LIGA is the acronym for “X-ray Lithographie Galvanoformung Abformung,” which means X-ray lithography, electrodeposition and molding. A dc voltage source was supplied across the electrodes to generate the distributed body force on the fluid in the pumping chamber. The external magnetic field was applied using permanent magnets. Different conducting solutions were used as the pumping fluids. Bubble generation affected the flow rates. Bubble generation was caused by electrolysis of the pumping fluids. Bubble generation could be reduced by reversing the direction of the applied voltage and ac driving mechanism would improve the performance.

Heng et al. [83] reported UV-LIGA microfabrication and test of an ac-type micropump based on the magnetohydrodynamic (MHD) principle. The microchannel material was glass substrate base with PMMA cover plate. A flow rate of 1900 $\mu\text{l}/\text{min}$ was achieved when ac voltage of 15 V was supplied at 1 Hz at 75 mA current. The magnetic flux density “ B ” was 2.1 T. Lemoff and Lee [85] proposed ac-type MHD micropump using anisotropic etching microfabrication process. Flow rates of 18.3 and 6.1 $\mu\text{l}/\text{min}$ were achieved when ac voltage of 25 V was supplied at 1 kHz.

5.2. Electrohydrodynamic (EHD)

The mechanism which allows the transduction of electrical to mechanical energy in an electrohydrodynamic (EHD) micropump is an electric field acting on induced charges in a fluid. The fluid flow in EHD micropump is thus manipulated by interaction of electric fields with the charges they induce in the fluid. One of the requirements of EHD micropumps is that the fluid must be of low conductivity and dielectric in nature. The electric body force density \vec{F} that results from an applied electric field with magnitude E is given as follows [86]:

$$\vec{F} = q\vec{E} + \vec{P}\nabla \cdot \vec{E} - \frac{1}{2}E^2\nabla \left[E^2 \left(\frac{\partial \epsilon}{\partial \rho} \right)_T \rho \right] \quad (10)$$

where q is the charge density, ϵ the fluid permittivity, ρ the fluid density, T the fluid temperature and \vec{P} is the polarization vector. A schematic geometry of EHD micropump is shown in Fig. 15.

The driving force of DC charged injection EHD micropump is the Coulomb force exerted on the charges between the two electrodes. EHD micropump requires two permeable electrodes in direct contact with the fluid to be pumped. Ions are injected from one or both electrodes into the fluid by electrochemical reactions. A pressure gradient develops between the electrodes and this leads to fluid motion between the emitter and the collector. The first DC charged injection EHD micropump was designed and fabricated by Ritcher et al. [86]. The micropump consisted of two electrically isolated grids. A flow rate of 15,000 $\mu\text{l}/\text{min}$ and a pressure head of around 1.72 kPa were reported at 800 V. The driving voltage could be reduced by reducing the grid distance.

Fuhr et al. [87] reported the first EHD micropump based on travelling wave-induced electroconvection. Waves of electric fields travelling perpendicular to the temperature and conductivity gradient, induce charges in the liquid. These charges interact with the travelling field and volume forces are generated to initiate fluid transport. In the EHD micropump design reported by Fuhr et al. [87], the electrode array was formed on the substrate and the flow channel was formed across the electrodes. The limitations of the earlier EHD micropumps were high voltage and liquid conductivity which must lie between 10^{-14} and 10^{-9} s/cm. The micropump reported in Ref. [87] showed that by using high frequency between 100 kHz to 30 MHz and low voltage between 20 and 50 V, liquids with conductivities between 10^{-4} and 10^{-1} s/cm could also be pumped. Flow in the range of 0.05–5 $\mu\text{l}/\text{min}$ was obtained.

Darabi et al. [88] reported an electrohydrodynamic (EHD) ion drag micropump. The dimensions of the micropump were

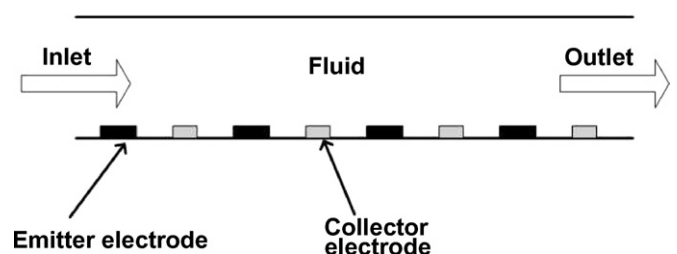


Fig. 15. Schematic geometry of EHD micropump.

19 mm × 32 mm × 1.05 mm. The driving mechanism was a combination of electrical field, dielectrophoretic force, dielectric force and electrostrictive force. The particles in dielectric fluid were charged by the applied electrical field so that the fluid was conveyed by induced electrostrictive forces. The electric field was developed by a pair of electrodes consisting of an emitter and a collector.

Badran et al. [89] investigated several designs of an electrohydrodynamic (EHD) ion drag micropump. The overall dimensions of the micropump channel were 500 μm × 80 μm × 60 μm. The effect of several design parameters such as different combinations of the gap between the electrodes on the pressure–voltage relationship were studied in this work. Darabi and Rhodes [90] reported on the computational fluid dynamics (CFD) modelling of ion drag electrohydrodynamic micropump. The simulations were done to numerically model EHD pumping to study the effects of electrode gap, stage gap, channel height, and applied voltage. It was found that for a given channel height there was an optimum d/g ratio at which the flow rate is maximum where ‘ d ’ is the stage gap and ‘ g ’ is the electrode gap.

5.3. Electroosmotic (EO)

Electroosmosis also called electrokinetic phenomenon, can be used to pump electrolyte solutions. In electroosmosis, an ionic solution moves relative to stationary, charged surfaces when electric field is applied externally. When an ionic solution comes in contact with solid surfaces, instantaneous electrical charge is acquired by the solid surfaces. For example, fused silica that is used commonly in the manufacturing of microchannels becomes negatively charged when an aqueous solution comes in contact with it. The negatively charged surface attracts the positively charged ions of the solution. When an external electric field is applied along the length of the channel, the thin layer of cation-rich fluid adjacent to the solid surfaces start moving towards the cathode. This boundary layer like motion eventually sets the bulk liquid into motion through viscous interaction. A sketch showing the electroosmotic pumping of fluid in a channel is presented in Fig. 16. Electroosmotic (EO) micropumps have certain advantages. An important one is that electroosmotic pumping does not involve any moving parts such as check valves. Standard and cheap MEMS techniques can be used for fabrication. The operation of electroosmotic micropump is quite. Flow direction in electroosmotic micropumps is controlled by switching the direction of the external electric field. The major limitations of electroosmotic micropumps are high voltage required and electrically conductive solution.

Zeng et al. [91] reported on the design and development of electroosmotic micropump fabricated by packing 3.5 μm non-porous silica particles into 500–700 μm diameter fused silica capillaries using silicate frit fabrication process. The micropump generated maximum pressure up to 2026.5 kPa and maximum flow rate of 3.6 μl/min at 2 kV applied voltage.

Chen and Santiago [92] reported a planar electroosmotic micropump. The micropump was fabricated using two pieces

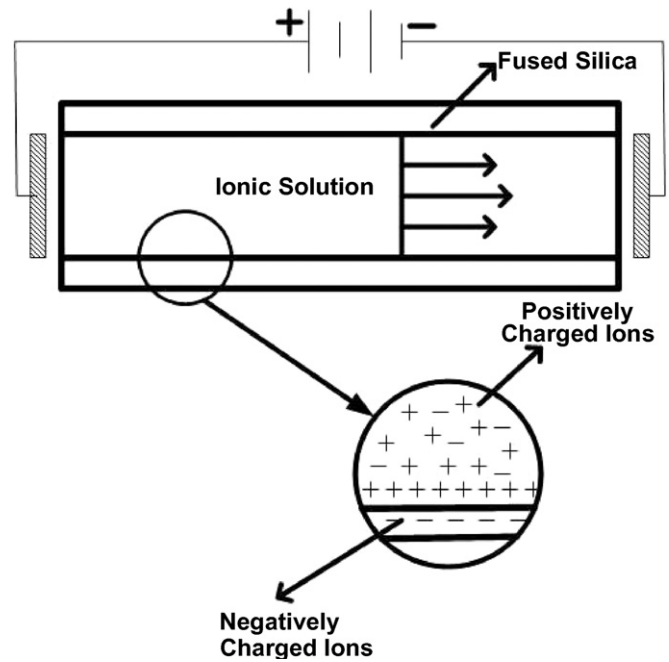


Fig. 16. Schematic illustration of electroosmotic flow in a channel.

of soda lime glass substrate. Standard microlithography techniques were used to generate photo resist etch masks. Chemical wet etching was used to fabricate the pumping channel and fluid reservoirs. The micropump generated a maximum pressure of 33 kPa and a maximum flow rate of 15 μl/min at 1 kV.

Chen et al. [93] reported on the development and characterization of multistage electroosmotic micropumps. A 1–3 stages electroosmotic micropumps were fabricated using 100 mm × 320 μm internal diameter columns packed with 2 μm porous silica particles, fused-silica capillaries and stainless electrodes. Compared to 1-stage electroosmotic micropump, the out pressures of 2 and 3 stage electroosmotic micropumps were two to three times higher and the flow rates of 2 and 3 stage electroosmotic micropumps were identical with that of the 1-stage micropump at the same driving voltage. Thus n -stage electroosmotic micropumps could be fabricated with potential applications in miniaturized fluid based systems such as micro-total analysis systems (μTAS).

Takemori et al. [94] reported a novel high-pressure electroosmotic micropump packed with silica nanospheres. A plastic chip was fabricated that confined uniform silica nanospheres within the channel to produce more efficient electroosmotic flow than the single microchannel with the same cross sectional area. The maximum flow rate of 0.47 μl/min and the maximum pressure of 72 kPa were achieved when 3 kV was applied to the electroosmotic pump.

Wang et al. [95] used silica-based monoliths with high charge density and high porosity for a high-pressure electroosmotic micropump having a diameter of 100 μm. The maximum flow rates and maximum pressure generated by the micropump using deionised water were 2.9 μl/min and 304 kPa respectively, at 6 kV applied voltage.

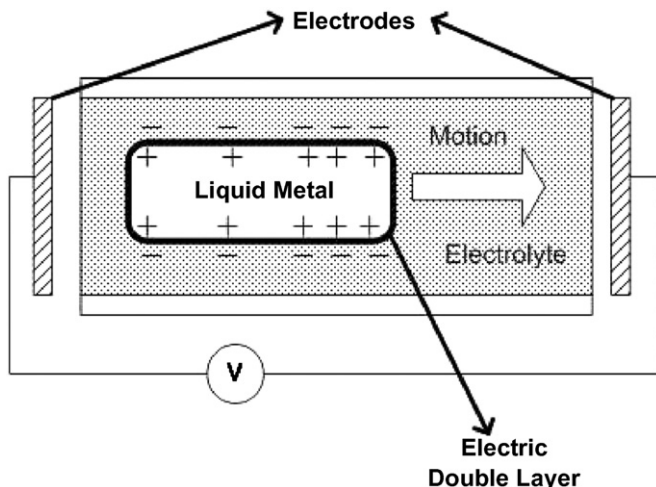


Fig. 17. Continuous electrowetting.

5.4. Electrowetting (EW)

Electrowetting involves wettability change due to applied electric potential. In electrowetting, the fluid is transported using surface tension. Surface tension is an interfacial force which dominates at microscale. Voltage is applied on the dielectric layer, decreasing the interfacial energy of the solid and liquid surface which results in fluid flow.

Continuous electrowetting (EW) is usually applied to adjust the surface tension between two immiscible liquids such as liquid-phased metal (e.g. mercury) and electrolyte. Its interface is referred to as “electric double layer” (EDL) as shown in Fig. 17. Due to protonation effect on the mercury surface, the electric potential between right end of mercury droplet and the cathode of electrode pair is higher than the counter electric potential on the left side. The surface tension difference beside a mercury droplet thus pushes the droplet toward right. Continuous electrowetting involves no heating of the liquid, demonstrate faster speed and low power consumption compared to thermo capillary.

Yun et al. [96] reported a continuous electrowetting (EW) micropump. Surface tension induced motion of mercury drop in a microchannel filled with electrolyte was used as the actuation energy for the micropump. The micropump was comprised of a stack of three wafers bonded together. The microchannel was formed on a glass wafer and filled with an electrolyte where the mercury drop was inserted. The movement of the mercury drop dragged the electrolyte which deflected the membrane formed on the second silicon wafer. The volumetric flow rate reached up to 70 $\mu\text{l}/\text{min}$ at driving voltage 2.3 V and power consumption of 170 μW . The maximum pressure was about 0.8 kPa by applying voltage of 2.3 V at 25 Hz frequency.

5.5. Bubble type

The pumping effect in bubble type micropumps is based on the periodic expansion and collapse of bubble generated in microchannel. A schematic illustration of expanding and collapsing bubble type micropump is shown in Fig. 18.

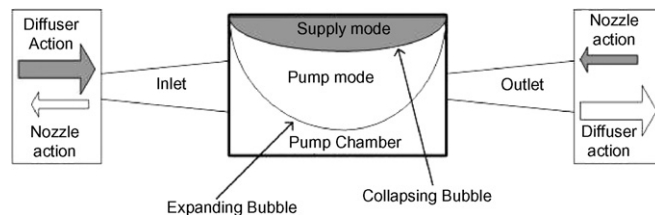


Fig. 18. A bubble micropump.

The bubble type micropumps always need to be heated so that their application scope is limited in case heating process is not allowed or preferred. Tsai and Lin [97] reported a valveless micropump based on thermal bubble actuation and nozzle/diffuser flow regulation. Microbubble was generated in the microchamber to create pumping chamber. Due to expansion of the bubble, the flow rate at the diffuser, Q_d was larger than the one at the nozzle, Q_n . When the pumping bubble collapsed, Q_d was smaller than Q_n . Thus a net flow was generated from nozzle to diffuser by periodically controlled voltage input during each cycle consisting of bubble expansion and collapse. The pumping chamber, nozzle/diffuser flow regulators and channels were fabricated on a silicon substrate. The maximum value of the flow rate of the bubble type micropump was 5 $\mu\text{l}/\text{min}$ as the applied voltage was exerted periodically at 250 Hz with 10% duty cycle and power consumption of 1 W.

Geng et al. [98] reported a bubble-based micropump for electrically conducting liquids. The device developed a head of a few millimeters of water with typical flow rates in the range of 100 $\mu\text{l}/\text{min}$. However high local temperature was observed due to a high AC voltage applied between two channels.

Zahn et al. [99] reported microneedles integrated with an on-chip MEMS bubble micropump for continuous drug delivery applications. The expansion and collapse of thermally generated bubbles with flow rectifying check valves were used to achieve the net flow rate through the device. The micropump was fabricated using silicon on insulator (SOI) fabrication process and quartz dice. Visual methods were used to record flow rates and net flow rate of water out of the microneedles was approximately 0.12 $\mu\text{l}/\text{min}$ with a pressure of 3.9 kPa. Drug delivery system such as reported in Ref. [99] with microneedles integrated with micropump, offers very tight control over injection flow rates at given drug concentrations. In addition such devices can also be used for sample collection for analysis. The flow direction can be reversed by reversing the valve direction and fluid can be extracted via micropump through microneedles. Thus such an integrated device can be used to determine glucose levels for diabetes patients.

Yin and Prosperetti [100] reported data obtained on a simple micropump based on the periodic growth and collapse of a single vapour bubble in a microchannel. The micropump was fabricated by laser machining of microchannel of 150 μm diameter on acrylic plate. The bottom plate was covered by another equal sized acrylic plate. Platinum wires were embedded in the grooves in the top plate to provide the heating source. For a channel diameter in the range of 100 μm , pumping rates of several tens of $\mu\text{l}/\text{min}$ and pressure differences of several kPa were

achieved by the system. The design of such type of micropumps was suitable for pumping electrically conducting fluids such as salts in some biomedical applications for which joule heating can be used to generate the bubble. Non-conducting fluids on the other hand require the use of heaters embedded in the microchannel. A preliminary demonstration of mixing effect was also presented by operating the micropump in parallel in two microchannels joined at a Y-junction. This could be potentially useful where two or more kinds of doses are required to be mixed up during the expanding/collapsing cycles.

Jung and Kwak [101] fabricated and tested a bubble-based micropump with embedded microheater. The micropump which consisted of a pair of valveless nozzle/diffuser elements and a pump chamber, was fabricated by embedding microheaters in a silicon dioxide layer on a silicon wafer which served as the base plate. The top plate of the micropump with inlet and outlet ports was made of glass wafer. The performance of the micropump was measured using deionised water. The applied square wave voltage pulse to the heater was 30 V. Volume flow rates were measured at 40, 50, 60, 70, and 80% duty ratios over the seven different operation frequencies from 0.5 to 2.0 Hz. An optimal flow rate of 6 $\mu\text{l}/\text{min}$ at 60% duty ratio for the circular chamber and 8 $\mu\text{l}/\text{min}$ at 40% duty ratio for the square chamber was measured which indicated that micropump flow rate decreased as the duty ratio increased.

5.6. Flexural planar wave (FPW) micropumps

In ultrasonically driven or flexural plate wave (FPW) micropumps, a phenomenon called acoustic streaming occurs in which a finite amplitude acoustic field is utilized to initiate the fluid flow. An array of piezoelectric actuators set the acoustic field by generating flexural planar waves which propagate along a thin plate. The thin plate forms one wall of the flow channel as shown in Fig. 19. There is momentum transfer from channel wall to the fluid.

Fluid motion by travelling flexural wave is used for the transport of liquids in an ultrasonically driven micropump. Flexural plate wave (FPW) micropump requires low operating voltage and there is no requirements of valves or heating. In contrast

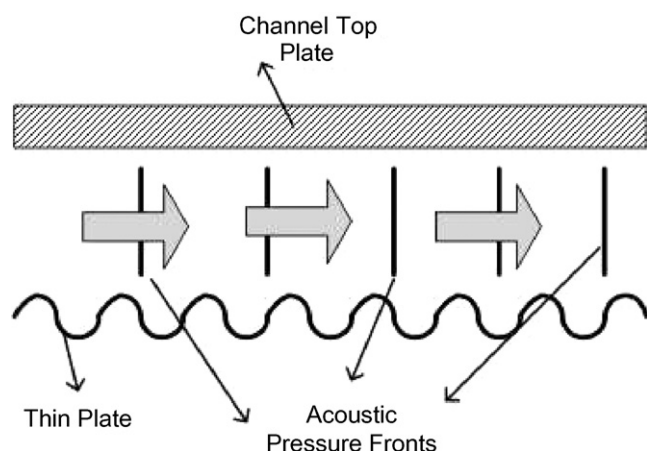


Fig. 19. Schematic illustration of acoustic streaming.

to the EHD micropumps, there is no limitation on the conductivity of liquids or gases. FPW pumping effect was reported by Moroney et al. [102]. Fluid motion was demonstrated when ultrasonic flexural waves propagated in thin membrane. Zinc oxide was used as piezoelectric layer to generate wave. A FPW micropump was reported by Luginbuhl et al. [103]. Piezoelectric zirconate titanate (PZT) sol–gel thin films were used as the piezoelectric layer. The device consisted of dual transducers patterned on a thin film composite membrane of silicon nitride and a sol–gel derived piezoelectric thin film. FPW actuator was used to pump liquids in silicon tubes with a flow rate of 0.255 $\mu\text{l}/\text{min}$. Nguyen et al. [104] proposed microfluidic system based on FPW micropump. The micropump was made of an aluminum, piezoelectric zinc oxide, polysilicon, and low-stress silicon nitride membrane with a typical thickness of 1–3 μm . The microfluidic system having a size of 10 mm \times 10 mm was fabricated using common fabrication techniques. The FPW micropump required low operating voltage and less power consumption (less than 10 mW). The micropump was suitable for delivering sensitive biomaterials. Potential applications include micrototal analysis system (μTAS), cell manipulating systems, and drug delivery systems.

Meng et al. [105] reported a micromachined micropump using ultrasonic flexural wave plate wave travelling along a thin membrane to excite an acoustic field in the fluid in contact with the membrane. The acoustic field generated the fluid flow. Bidirectional and focused flow was achieved by a novel combination of radial transducers. Potential applications of this type of micropumps include micrototal analysis systems and drug delivery devices.

5.7. Electrochemical

In electrochemical micropumps, the electrochemical generation of gas bubbles by the electrolysis of water, provides the driving force to dispense liquids. Thus electrochemical micropump utilizes the bubble force that is generated by electrochemical reaction during electrolysis. The structure of the micropump is composed of electrodes for supplying electricity, fluid channels, chamber for electrolysis (bubble generation) and inlet and outlet reservoirs. A schematic illustration of electrochemical actuation is shown in Fig. 20. The design and construction of the electrochemical micropump is relatively simple and it can be easily integrated with other microfluidic systems. The limitation of the electrochemical micropump is that the generated bubble might collapse and become water leading to unsteady and unreliable release of drug.

Bohm et al. [106] reported an electrochemically actuated micropump for closed loop controlled microdosing system. Electrochemical generation of gas bubbles by electrolysis of water provided the driving force to dispense the fluid. The dosing system comprised of a micromachined channel and reservoir structure made of silicon and pyrex cover on which a set of platinum electrodes were patterned. The electrodes were used for electrochemical gas generation. The rate of bubble generation was about 0.0012 $\mu\text{l}/\text{min}$.

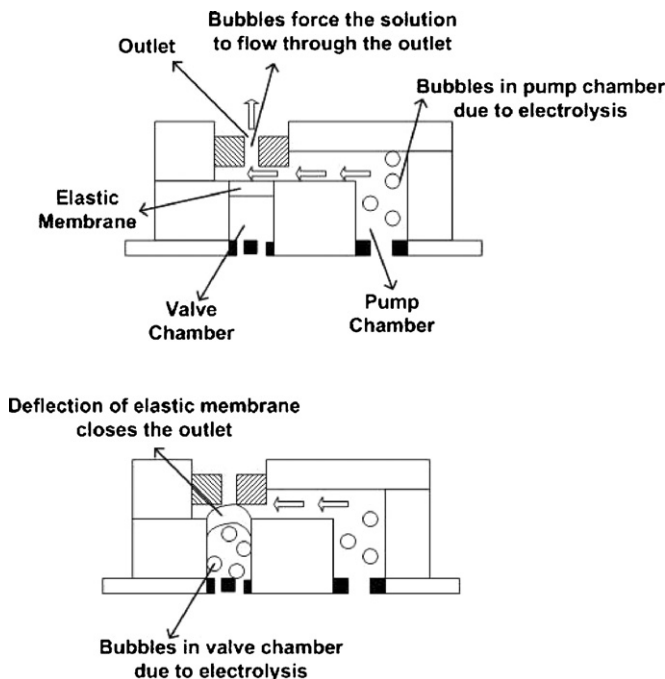


Fig. 20. Schematic illustration of electrochemical actuation.

Suzuki and Yoneyama [107] proposed a reversible electrochemical nano syringe pump. The micropump was fabricated by micromachining. Thin film three electrode system for actuation and sensing was formed on a glass substrate. Microchannel and reservoir for electrolyte were formed on the silicon substrate. The micropump operated at constant potential using hydrogen bubble as the working medium. Pumping rate was controlled by setting the applied potential of the working electrode to an appropriate value. The micropump could be used to pump external solution into and out of the system as well as pumping internal solution out of the system as required in drug delivery systems.

Yoshimi et al. [108] developed a method of chemical stimulation of neurons using a neurotransmitter containing an electrochemical micropump. The electrochemical micropump was powered by the bubble generated during water electrolysis. The micropump consisted of a glass nozzle with 10 μm diameter tip. Two platinum electrodes for electrolysis were embedded in the pump body which was filled with neurotransmitter solution. A potential difference of 3 V was applied to the electrodes to direct the solution to flow towards the neurons. The micropump was capable of rapid administration of neurotransmitters to neurons. The micropump design could be miniaturized to create “synapses” in artificial sensory organs.

Kabata and Suzuki [109] developed a micropump based on electrochemical principle for micro insulin injection system. Major components of the micropump were a thin film two-electrode system in a closed compartment, a silicone rubber diaphragm to separate an electrolyte solution from an insulin solution, and a reservoir for insulin. A microneedle was attached to the outlet. The hydrogen bubbles are generated on the working electrode. This resulted in deformation of the diaphragm, and the insulin solution was pumped out through the microneedle.

5.8. Evaporation type

The pumping principle of an evaporation-based micropump is similar to the xylem transport system in trees. The design principle of the micropump involves controlled evaporation of a liquid through a membrane into a gas space containing a sorption agent. A schematic illustration of the micropump is shown in Fig. 21.

Effenhauser et al. [110] reported an evaporation-based disposable micropump concept that has potential applications in continuous patient monitoring systems. The vapour pressure in the gas chamber was kept below saturation and during this phase, fluid evaporation from the membrane was replaced by capillary forces which induced flow from the reservoir. Evaporated liquid was continuously replaced by flow of liquid through the microfluidic system such as microdialysis catheter. The average flow rate of 0.35 $\mu\text{l}/\text{min}$ was achieved. Low fabrication cost, no moving parts and lack of external energy source were important features of this type of micropump. The main drawback of the pump was that it worked only in suction mode. Such type of micropumps can be used for continuous glucose monitoring where a dialysis solution is pumped in a constant fashion at small flow rates through a microfluidic system such as microdialysis catheter.

Namasivayam et al. [111] investigated transpiration-based micropump for delivering continuous ultra low flow rates. The pumping concept was based on the commonly observed phenomenon of transpiration in plant leaves. When the liquid was heated at the meniscus, the vapour pressure increased resulting in enhanced evaporation. As the vapour diffused out, a fresh liquid supply was drawn into the channel from a reservoir for steady state operation. The capillary force aided imbibition process (absorption or adsorption of liquid) continued until the reservoir was depleted after which the meniscus began to draw back.

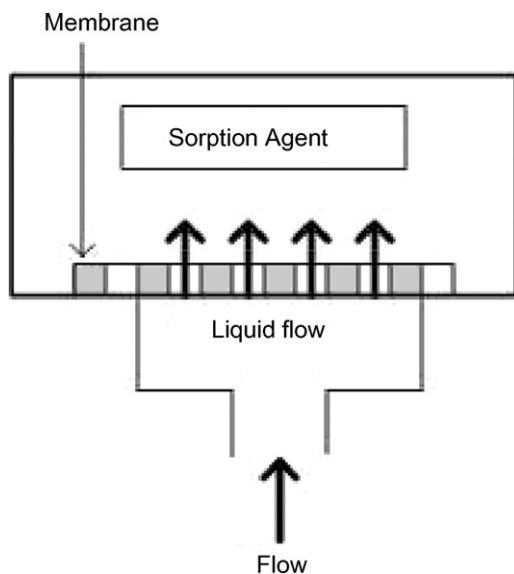


Fig. 21. Schematic illustration of evaporation based micropump.

6. Discussion

The fabricated structure of most of the mechanical and non-mechanical micropumps reported above is composed of glass, silicon or plastic. However in view of the increased use of MEMS-based micropumps in implantable drug delivery systems and emphasis on lowering the manufacturing costs, silicon is now being replaced with polymer based materials such as polydimethylsiloxane (PDMS) and polymethylmethacrylate (PMMA), etc. The use of polymer based materials is rapidly growing because of their good biocompatibility, excellent physical and mechanical properties, low cost and simple and fast fabrication.

Various factors other than pressure and flow rate are relevant to the selection of mechanical micropump. The magnitude of applied voltage required for these micropumps is one of the important factors which can be compared directly and which varies widely. Voltage is an important parameter of micropump as it determines the electronics and other components to operate the micropump. In Fig. 22, graphical representation of flow rates and operating voltages for reported mechanical micropumps is shown. The values of flow rate and voltage are plotted on a log scale to facilitate comparison. Electrostatic, piezoelectric and thermopneumatic micropumps produce higher flow rates at the expense of high-applied voltage values. Micropumps with conducting polymer film actuators such as ICPF appear to be the most promising mechanical micropumps which provide adequate flow rates at very low applied voltage. Bimetallic micropumps also require less voltage and provide higher flow rates.

As with mechanical micropumps, performance of non-mechanical micropumps is also dependent on various other

factors in addition to pressure and flow rate. In Fig. 23, graphical representation of flow rates and operating voltages for reported non-mechanical micropumps is shown. The values of flow rate and voltage are plotted on a log scale to facilitate comparison. Electroosmotic micropumps require high operating voltages and produce low flow rates. Electroosmotic micropumps are generally used in microanalysis systems where low flow rates are required. MHD and EHD micropumps produce high flow rates at the expense of high operating voltages. Electrowetting and electrochemical type of micropump are the most promising ones which exhibit high flow rate at low applied voltage. Working fluid properties also influence the flow rates and must be taken into account in choosing non-mechanical micropumps. Electroosmotic and magnetohydrodynamic micropumps can handle many working fluids which are widely used in chemical and biological analysis. Electrochemical micropumps can also handle a variety of solutions such as insulin and neurotransmitter solution in drug delivery application.

Flow rate, pressure generated and size of the micropumps are important parameters of micropumps. Another important parameter is the ratio of micropump flow rate to its size which is referred to as self pumping frequency [8]. To compare mechanical and non-mechanical micropumps, self-pumping frequency was calculated for micropumps where both the size and flow rates were available in addition to pressure. In Fig. 24, comparison of mechanical and non-mechanical micropumps in terms of size, self-pumping frequency and flow rates is presented. Pressure values of the micropumps are plotted in Fig. 25.

Size of the micropump is an important parameter as it influences the particular application of a micropump. The different manufacturing processes and operational nature of mechani-

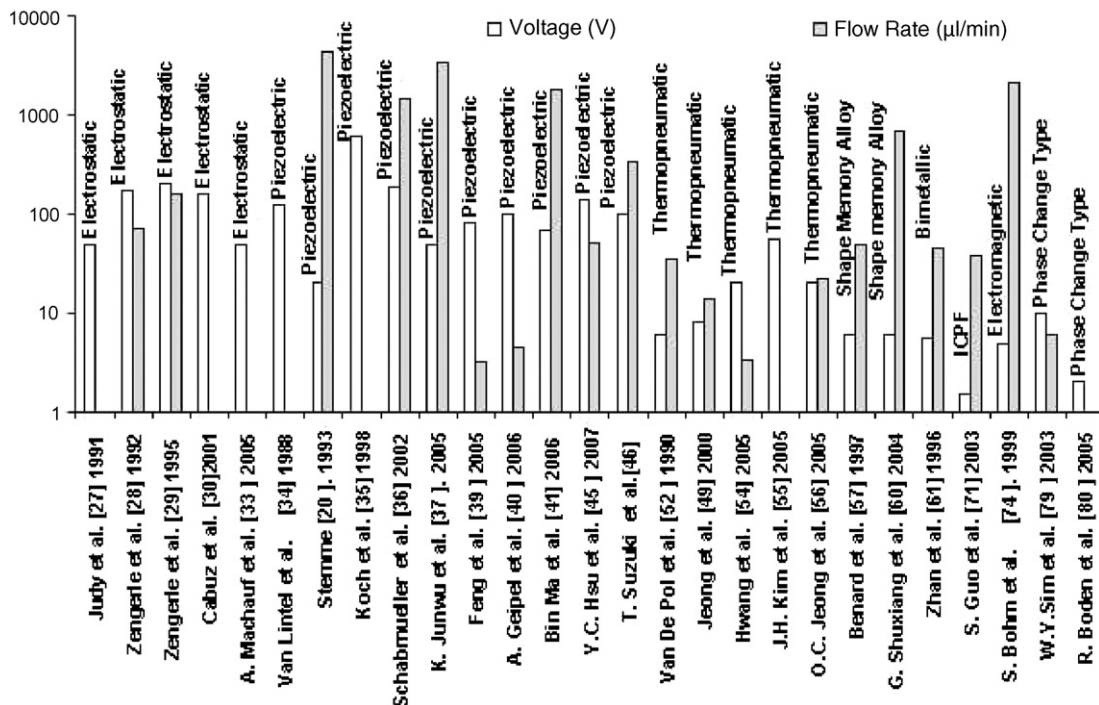


Fig. 22. Comparison of voltage vs. flow rate for mechanical micropumps.

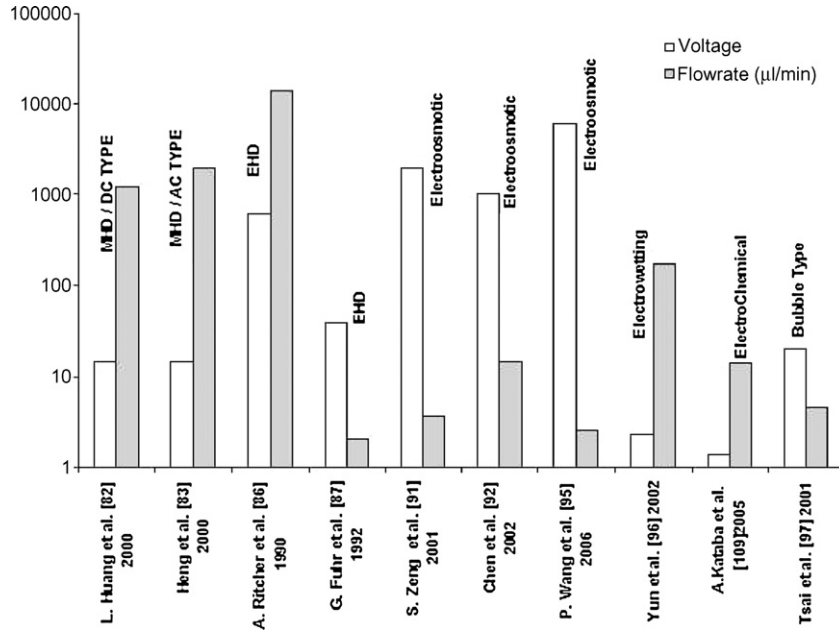


Fig. 23. Comparison of voltage vs. flow rate for non-mechanical micropumps.

cal and non-mechanical micropumps generally dictate which micropump is suitable for a particular application. Electroosmotic pump reported by Zeng et al. [91] which is smaller in size as compared to electroosmotic micropump reported by Chen and Santiago [92], performs better in terms of pressure generation as shown in Figs. 24 and 25, respectively. Therefore electroosmotic pump reported by Zeng et al. [91] is intended for applications where compactness in terms of size is required along with high-pressure generation. Thermopneumatic micropumps such as the one reported by Van De Pol et al. [52] tend to produce low flow rates and low pressures relative to their size. However their

performance must be measured against low cost manufacturing associated with these micropumps. Piezoelectric micropump reported by Stemme and Stemme [20] performs better in terms of flow rate achieved with relatively better self-pumping frequency and smaller size as compared to the piezoelectric micropump reported by Van Lintel et al. [34]. Among all micropumps compared in Fig. 24, piezoelectric micropump reported by Schabmueller et al. [36] exhibits the highest self-pumping frequency and adequate flow rate with respect to its small size. Bimetallic micropumps such as the one reported by Zou et al. [63] exhibit higher self-pumping frequency and high flow rate at rel-

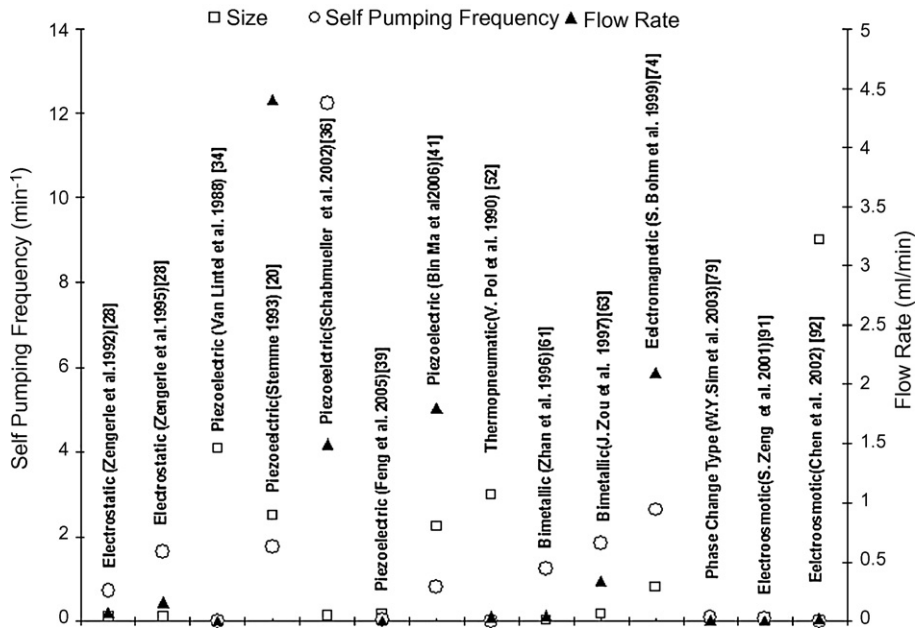


Fig. 24. Comparison of mechanical and non-micropumps in terms of size, flow rate and self pumping frequency.

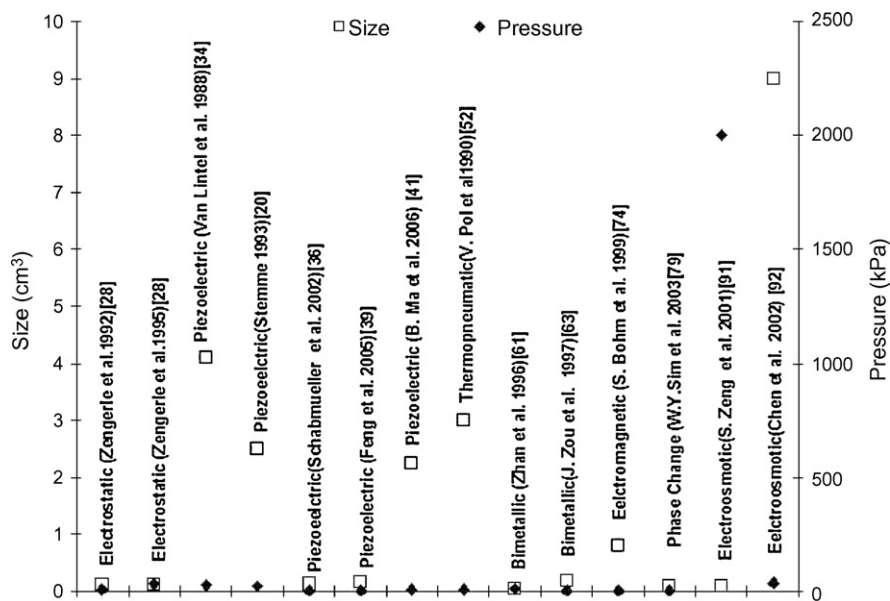


Fig. 25. Comparison of mechanical and non-micropumps in terms of size and pressure.

atively smaller size of the micropump. Similarly, electrostatic micropump reported by R. Zengerle et al. [28] exhibits high self-pumping frequency at a small size of the micropump. Therefore further research on bimetallic and electrostatically actuated micropumps is suggested to further improve the performance of mechanical micropumps. Non-mechanical Electroosmotic [91] and mechanical electrostatic [27–28] and piezoelectric micropumps [39] of comparable sizes show comparable performance in terms of flow rates.

7. Conclusion

The pioneering work on micropumps started in 1975. However research and development on micropumps using microfabrication technology started in 1980s and shifted towards MEMS area around 1990. Since then, MEMS technologies have been applied to the needs of biomedical industry, resulting in development of various categories of micropump concepts, fabrication technologies, devices and applications. Micropumps for various biomedical applications such as transdermal insulin delivery, artificial sphincter prosthesis, antithrombogenic micropumps for blood transportation, micropump for injection of glucose for diabetes patients and administration of neurotransmitters to neurons and micropumps for chemical and biological sensing have been reported. Biocompatibility of MEMS-based micropumps is becoming increasingly important and use of biocompatible polymer based materials such as polydimethylsiloxane (PDMS) and polymethylmethacrylate (PMMA), etc. is growing. Piezoelectrically actuated mechanical displacement micropumps have been the focus of particular attention and have been widely used in drug delivery and point of care testing (POCT) systems. The applied voltage is a key constraint factor for drug delivery driving power. In other words, the micropumps have to be limited by low applied voltage because of their critical appli-

cation in drug delivery systems. Electrostatic and piezoelectric micropumps require high driving voltage. Micropumps with conducting polymer film actuators such as ICPF appear to be the most promising mechanical micropumps which provide adequate flow rates at very low applied voltages. However their performance must be weighed against complex and difficult batch fabrication. Among non-mechanical micropumps, electrowetting and electrochemical type of micropump are suitable for low voltage and high flow rate applications. Electroosmotic micropumps require high operating voltages and exhibit low flow rates. Such types of micropumps are suitable for applications in micro-analysis systems. Based on the extensive literature review, the authors conclude that overall commercialization of MEMS micropumps in drug delivery and biomedical application is still in its beginning. A lot of technical information is available for a number of micropump concepts. However many of the novel micropumps reported in literature for drug delivery and other biomedical applications still need to be incorporated into practical devices. To find a micropump suitable for a particular application is a challenge and this will continue to motivate researchers to work on developing micropumps and incorporating them in practical drug delivery and biomedical systems.

Acknowledgements

The authors would like to thank and acknowledge National Electronics and Computer Technology Center, Thailand for providing the grant under the MEMS project.

References

- [1] R.S. Shawgo, A.C. Richards Grayson, L. Yawen, et al., BioMEMS for drug delivery, *Curr. Opin. Solid-State Mater. Sci.* 6 (2002) 329–334.

- [2] S.L. Tao, T.A. Desai, Microfabricated drug delivery systems: from particles to pores, *Adv. Drug Delivery Rev.* 55 (2003) 315–328.
- [3] X.Z. Zhang, R.X. Zhou, J.Z. Cui, et al., Microcontrolled release, *Int. J. Pharmaceut.* 235 (2002) 43–50.
- [4] D.L. Polla, BioMEMS applications in medicine, in: *International Symposium on Microelectronics and Human Science*, vol. 0-7803-7190-9/01, 2001, pp. 13–15.
- [5] S.R. Shawgo, C. Amy, R. Grayson, Li. Yawen, J. Michael Cima, BioMEMS for drug delivery, *Curr. Opin. Solid-State Mater. Sci.* 6 (2002) 329–334.
- [6] C. Amy, R. Grayson, R. Scheidt Shawgo, Y. Li, M.J. Cima, Electronic MEMS for triggered delivery, *Adv. Drug Delivery Rev.* 56 (2004) 173–184.
- [7] M. Staples, K. Daniel, M.J. Cima, R. Langer, Application of micro and nano electromechanical devices to drug delivery, *Pharm. Res.* 23 (5) (2006) 847–863.
- [8] D.J. Laser, J.G. Santiago, A review of micropumps, *J. Micromech. Microeng.* 14 (2004) 35–64.
- [9] P. Woias, Micropumps-past, progress and future prospects, *Sens. Actuators B: Chem.* 105 (2005) 28–38.
- [10] N.C. Tsai, C.Y. Sue, Review of MEMS based drug delivery and dosing systems, *Sens. Actuators A: Phys.* 134 (2007) 555–564.
- [11] F. Tay, *Microfluidics and BioMEMS Applications*, 1st ed., Springer, Kluwer Academic Publishers, Boston, 2002, pp. 3–24, ISBN: 1402072376.
- [12] L.J. Thomas Jr., S.P. Bessman, Micropump powered by piezoelectric disk benders, US patent 3,963,380, USA, 1975.
- [13] J.G. Smits, Piezoelectrical micropump, European patent EP0134614, Netherlands, 1984.
- [14] J.G. Smits, Piezoelectric micropump with three valves working peristaltically, *Sens. Actuators A: Phys.* 21 (1–3) (1990) 203–206.
- [15] K. Kamper, P. Dopfer, J. Ehrfeld, W.S. Oberbeck, A self-filling low cost membrane micropump, in: *Proceedings of the 11th Annual International Workshop on Microelectromechanical Systems*, Heidelberg, Germany, 1998.
- [16] H.Q. Li, et al., A high frequency high flow rate piezoelectrically driven MEMS micropump, in: *Proceedings of the Solid State Sensor and Actuator Workshop*, Hilton Head, SC, 2000.
- [17] K. Sato, M. Shikida, An electrostatically actuated gas valve with an S-shaped film element, *J. Micromech. Microeng.* 4 (1994) 205–209.
- [18] J. Fahrenberg, et al., A microvalve system fabricated by thermoplastic molding, *J. Micromech. Microeng.* 5 (1995) 169–171.
- [19] M. Esashi, S. Shoji, A. Nakano, Normally closed microvalve and micropump fabricated on a silicon wafer, *Sens. Actuators* 20 (1989) 163–169.
- [20] E. Stemme, G. Stemme, A valveless diffuser/nozzle-based fluid pump, *Sens. Actuators A: Phys.* 39 (2) (1993) 159–167.
- [21] G. Lins, L. Skogberg, An Investigation of Insulin Pump Therapy and Evaluation of Using a Micropump in a Future Insulin Pump, M.S. thesis, KTH, Stockholm, Sweden, 2001.
- [22] C. Amy, et al., A BioMEMS review: MEMS technology for physiologically integrated devices, in: *Proceedings of the IEEE* 92 1, 2004, pp. 6–21.
- [23] J.M. Anderson, J.J. Langone, Issues and perspectives on the biocompatibility and immunotoxicity evaluation of implanted controlled release systems, *J. Control Release* 57 (2) (1999) 107–113.
- [24] J.M. Anderson, *Inflammation, Wound Healing and the Foreign Body Response Biomaterials Science: An Introduction to Materials in Medicine*, Academic Press Inc., San Diego, CA, 1996 (Chapter 4 (4.2)).
- [25] F.M. White, *Fluid Mechanics*, International student ed., McGraw Hill Inc., 1979, pp. 161–162.
- [26] E. Meng, MEMS Technology and Device for a Microfluid Dosing System, PhD thesis, California Institute of Technology, 2003.
- [27] J.W. Judy, T. Tamagawa, D.L. Polla, Surface micromachined micropump, *Proc. MEMS* 91 (1991) 182–186.
- [28] R. Zengerle, M. Richter, H. Sandmaier, A micro membrane pump with electrostatic actuation, in: *Proceedings of IEEE, Microelectromechanical System*, 1992, pp. 19–24.
- [29] R. Zengerle, J. Ulrich, S. Kluge, M. Richter, A. Richter, A bidirectional silicon micropump, *Sens. Actuators A* 50 (1995) 81–86.
- [30] C. Cabuz, W.R. Herb, E.I. Cabuz, S.T. Lu, The dual diaphragm pump, in: *Proceedings of the IEEE MEMS*, 2001, pp. 519–522.
- [31] M.M. Teymoori, A.A. Sani, Design and simulation of a novel electrostatic micromachined pump for drug delivery applications, *Sens. Actuators A: Phys.* 117 (2005) 222–229.
- [32] T. Bourouinay, B. Alain, J.P. Grandchamp, Design and simulation of an electrostatic micropump for drug delivery applications, *J. Micromech. Microeng.* 7 (1997) 186–188.
- [33] A. Machauf, Y. Nemirovsky, U. Dinnar, A membrane micropump electrostatically actuated across the working fluid, *J. Micromech. Microeng.* 15 (2005) 2309–2316.
- [34] H.T.G. Van Lintel, F.C.M. van De Pol, S. Bouwstra, A piezoelectric micropump based on micromachining of silicon, *Sens. Actuators*. 15 (2) (1988) 153–167.
- [35] M. Koch, N. Harris, A.G.R. Evans, N.M. White, A. Brunnschweiler, A novel micromachined pump based on thick film piezoelectric actuation, *Sens. Actuators A: Phys.* 70 (1998) 98–103.
- [36] C.G.J. Schabmueller, M. Koch, M.E. Mokhtari, A.G.R. Evans, A. Brunnschweiler, H. Sehr, Self-aligning gas/liquid micropump, *J. Micromech. Microeng.* 12 (2002) 420–424.
- [37] K. Junwu, Y. Zhigang, P. Taijiang, C. Guangming, W. Boda, Design and test of a high performance piezoelectric micropump for drug delivery, *Sens. Actuators A: Phys.* 121 (2005) 156–161.
- [38] S.W. Lee, W.Y. Sim, S.S. Yang, Fabrication and invitro test of a microsyringe, *Sens. Actuators A: Phys.* 83 (2000) 17–23.
- [39] G.H. Feng, E.S. Kim, Piezoelectrically actuated dome-shaped diaphragm micropump, *J. Microelectromech. Syst.* 14 (2005) 192–199.
- [40] A. Geipel, A. Doll, F. Goldschmidtboing, P. Jantscheff, N. Esser, U. Massing, P. Woias, Pressure independent micropump with piezoelectric valves for low flow drug delivery systems, *MEMS 2006*, Istanbul, Turkey, 22–26 January, 2006.
- [41] B. Ma, L. Sheng, Z. Gan, G. Liu, X. Cai, H. Zhang, Z. Yang, A PZT insulin pump integrated with a silicon micro needle array for transdermal drug delivery, in: *Proceedings of the 56th Electronic Components and Technology Conference*, 2006, pp. 677–681.
- [42] A. Doll, M. Heinrichs, F. Goldschmidtboeing, H.J. Schrag, U.T. Hopt, P. Woias, A high performance bidirectional micropump for a novel artificial sphincter system, *Sens. Actuators A* 130/131 (2006) 445–453.
- [43] H.J. Schrag, German Patent DE10,023,634, 2003.
- [44] H.J. Schrag, F.F. Padilla, F. Goldschmidtboeing, A. Doll, P. Woias, U.T. Hopt, German Artificial Sphincter System, GASS, first report of a novel and highly integrated sphincter prosthesis for the therapy of major fecal incontinence, *Biomed. Technol.* 49 (2004) 274–278.
- [45] Y.C. Hsu, S.J. Lin, C.C. Hou, Development of peristaltic antithrombotic micropumps for in vitro and ex vivo blood transportation tests, *Microsystem Technologies*, Springer-Verlag 14 (2008) 31–41.
- [46] T. Suzuki, Y. Teramura, H. Hata, K. Inokuma, I. Kanno, H. Iwata, H. Kotera, Development of a micro biochip integrated travelling wave micropumps and surface plasmon resonance imaging sensors, *Microsystem Technologies*, Springer-Verlag 13 (2007) 1391–1396.
- [47] R. Linnemann, C. Woias, J.A. Senfft, R. Linnemann, Ditterich A self priming and bubble tolerant silicon micropump for liquids and gases, in: *Proceedings of the MEMS*, 98, Heidelberg, Germany, 1998, pp. 532–537.
- [48] C.J. Morris, F.K. Forster, Optimization of a circular piezoelectric bimorph for a micropump driver, *J. Micromech. Microeng.* 10 (2000) 459–465.
- [49] O.C. Jeong, S.S. Yang, Fabrication and test of a thermopneumatic micropump with a corrugated p+diaphragm, *Sens. Actuators A: Phys.* 83 (2000) 249–255.
- [50] S. Zimmermann, J.A. Frank, D. Liepmann, A.P. Pisano, A planar micropump utilizing thermopneumatic actuation and in-plane flap valves, in: *Proceedings of the 17th IEEE International Conference on Micro Electro Mechanical Systems (MEMS): MEMS 2004 Technical Digest*, Maasricht, 2004, pp. 462–465.

- [51] W.K. Schomburg, J. Vollmer, B. Bustgens, J. Fahrenberg, H. Hein, W. Menz, Microfluidic components in LIGA technique, *J. Micromech. Microeng.* 4 (1994) 186–191.
- [52] F.C.M. Van De Pol, H.T.G. Van Lintel, M. Elwenspoeck, J.H.J. Fluitman, A thermopneumatic micropump based on microengineering techniques, *Sens. Actuators A: Phys.* 21 (1990) 198–202.
- [53] M.J. Zdelblich, J.B. Angell, A microminiature electric to fluidic valve, in: *Proceedings of the 4th International Conference Solid State Sensors and Actuators (Transducer '87)*, Tokyo, Japan, 1987, p. 827.
- [54] S.R. Hwang, W.Y. Sim, D.H. Jeon, G.Y. Kim, S.S. Yang, J.J. Pak, Fabrication and test of a submicroliter level thermopneumatic micropump for transdermal drug delivery, in: *Proceedings of the 3rd Annual International IEEE EMBS Special Topic Conference on Microtechnologies in Medicine and Biology*, Kahuku, Oahu, Hawaii, 2005.
- [55] J.H. Kim, K.H. Na, C.J. Kang, Y.S. Kima, A disposable thermopneumatic actuated micropump stacked with PDMS layers and ITO coated glass, *Sens. Actuators A: Phys.* 120 (2005) 365–369.
- [56] O.C. Jeong, S.W. Park, S.S. Yang, J.J. Pak, Fabrication of a peristaltic PDMS micropump, *Sens. Actuators A: Phys.* 123/124 (2005) 453–458.
- [57] W.L. Benard, H. Kahn, A.H. Heuer, M.A. Huff, A titanium–nickel shape memory alloy actuated micropump, in: *International Conference on Solid State Sensors and Actuators*, vol. 1, 1997, pp. 361–364.
- [58] W.L. Benard, H. Kahn, A.H. Heuer, M.A. Huff, Thin film shape memory alloy actuated micropumps, *J. MEMS* 7 (1998) 245–251.
- [59] D. Xu, L. Wang, G. Ding, Y. Zhou, A. Yu, B. Cai, Characteristics and fabrication of NiTi/Si diaphragm micropump, *Sens. Actuators A: Phys.* 93 (2001) 87–92.
- [60] G. Shuxiang, T. Fukuda, SMA actuator based novel type of micropump for biomedical application, in: *IEEE International Conference*, vol. 2, 2004, pp. 1616–1621.
- [61] C. Zhan, T. Lo, L.P. Liu, A silicon membrane micropump with integrated bimetallic actuator, *Chinese J. Electron.* 5 (1996) 29–35.
- [62] Y. Yang, Z. Zhou, X. Ye, X. Jiang, Bimetallic Thermally Actuated Micropump, vol. 59, American Society of Mechanical Engineers, Dynamic Systems and Control Division (Publication) DSC, 1996, pp. 351–354.
- [63] J.X. Zou, Y.Z. Ye, Y. Zhou, Y. Yang, A novel thermally actuated silicon micropump, in: *Proceedings of the 1997 International Symposium on Micromechanics and Human Science*, October, 1997, pp. 231–234.
- [64] J. Pang, Q. Zou, Z. Tan, X. Qian, L. Liu, Z. Li, The study of single chip integrated microfluidic system, in: *Proceedings of 5th International Conference on Solid State and Integrated Circuit Technology*, October, 1998, pp. 895–898.
- [65] S. Guo, T. Fukuda, K. Asaka, A new type of fish like underwater micro-robot, in: *Proceedings of the IEEE/ASME Transactions on Mechatronics*, vol. 8, no. 1, 2003.
- [66] S. Guo, T. Fukuda, K. Kosuge, F. Arai, M. Negoro, Micro catheter system with active guide wire, in: *Proceedings of the IEEE international Conference on Robotics and Automation*, 1995, pp. 79–84.
- [67] S. Tadokoro, S. Yamagami, M. Ozawa, Soft micromanipulation device with multiple degrees of freedom consisting of high polymer gel actuators, in: *Proceedings of the IEEE International Conference on Microelectromechanical Systems*, 1999, pp. 37–42.
- [68] S. Guo, T. Nakamura, T. Fukuda, K. Oguro, Design and experiments of micropump using ICPF actuator, in: *Proceedings of the Seventh International IEEE Symposium on Micro Machine and Human Science*, vol. 0-7803-3596-1/96, 1996, pp. 235–240.
- [69] S. Guo, T. Fukuda, Development of the micropump using ICPF actuator, in: *Proceedings of IEEE International Conference on Robotics and Automation*, vol. 1, 1997, pp. 266–271.
- [70] S. Guo, K. Sugimoto, T. Fukuda, K. Oguro, New type of capsule medical micropump, in: *IEEE/ASME International Conference on Advanced Intelligent Mechatronics (AIM)*, 1999, pp. 55–60.
- [71] S. Guo, K. Asaka, Polymer based new type of micropump for biomedical applications, in: *Proceedings of the IEEE Conference on Robotics & Automation Taipei, Taiwan*, 2003, pp. 1830–1835.
- [72] S. Guo, N. Kato, T. Fukuda, K. Oguro, A fish microrobot using ICPF Actuator, in: *Proceedings of the 5th International Workshop on Advanced Motion Control, AMC'98*, Coimbra, Portugal, 1998, pp. 592–597.
- [73] S. Guo, K. Wakubayashi, N. Kato, T. Fukuda, T. Nakamura, K. Oguro, An artificial fish robot using ICPF actuator, in: *International IEEE Symposium on Micromechanics and Human Science*, vol. 0-7803-4171-6/97, 1997.
- [74] S. Bohm, W. Olthuis, P. Bergveld, A plastic micropump constructed with conventional techniques and materials, *Sens. Actuators A: Phys.* 77 (1999) 223–228.
- [75] Q. Gong, Z. Zhou, Y. Yang, X. Wang, Design, optimization and simulation of microelectromagnetic pump, *Sens. Actuators A: Phys.* 83 (2000) 200–207.
- [76] C. Yamahata, C. Lotto, E. Al Assaf, M.A.M. Gijs, A PMMA valveless micropump using electromagnetic actuation, *Microfluid Nanofluid* 1 (2005) 197–207.
- [77] C. Yamahata, M. Chastellain, V.K. Parashar, A. Petri, H. Hofmann, M.A.M. Gijs, Plastic Micropump with ferrofluidic actuation, *J. Microelectromech. Syst.* 14 (2005) 96–102.
- [78] T. Pan, S.J. McDonald, E.M. Kai1, B. Ziaie1, A magnetically driven PDMS micropump with ball check valves, *J. Micromech. Microeng.* 15 (2005) 1021–1026.
- [79] W.Y. Sim, H.J. Yoon, O.C. Jeong, S.S. Yang, A phase change type of micropump with aluminum flap valves, *J. Micromech. Microeng.* 13 (2003) 286–294.
- [80] R. Boden, M. Lehto, U. Simu, G. Thornell, K. Hjort, J.A. Schweitz, A polymeric paraffin micropump with active valves for high pressure microfluidics, in: *Proceedings of the 13th International Conference on Solid State Sensors, Actuators and Microsystems*, Seoul, Korea, 2005, pp. 201–204.
- [81] J. Jang, S.S. Lee, Theoretical and experimental study of MHD (magneto-hydrodynamic) micropump, *Sens. Actuators A: Phys.* 80 (2000) 84–89.
- [82] L. Huang, W. Wang, M.C. Murphy, K. Lian, Z.G. Ling, LIGA fabrication and test of a DC type magnetohydrodynamic (MHD) micropump, *Microsyst. Technol.* 6 (2000) 235–240.
- [83] K.H. Heng, W. Wang, M.C. Murphy, K. Lian, UV-LIGA microfabrication and test of an AC-type micropump based on the magnetohydrodynamic (MHD) principle, *Proceedings of the SPIE-Microfluidic Dev. Syst.* III 4177, 2000, pp. 174–184.
- [84] J.C.T. Eijel, C. Dalton, C.J. Hayden, J.P.H. Burt, A. Manz, A circular AC magnetohydrodynamic micropump for chromatographic applications, *Sens. Actuators B: Chem.* 92 (2003) 215–221.
- [85] A.V. Lemoff, A.P. Lee, An AC magnetohydrodynamic micropump, *Sens. Actuators B: Chem.* 63 (2000) 178–185.
- [86] A. Richter, H. Sandmaier, An electrohydrodynamic micropump, in: *Proceedings of IEEE, Microelectromechanical Systems*, 1990, pp. 99–104.
- [87] G. Fuhr, R. Hagedorn, T. Muller, W. Benecke, B. Wagner, Pumping of water solutions in microfabricated electrohydrodynamic systems, in: *Proceedings of IEEE MEMS '92*, 1992, pp. 25–30.
- [88] J. Darabi, M. Rada, M. Ohadi, J. Lawler, Design, fabrication, and testing of an electrohydrodynamic ion drag micropump, *J. Microelectromech. Syst.* 11 (2002) 684–690.
- [89] M. Badran, M. Moussa, On the design of an electrohydrodynamic ion drag micropump, *Proceedings of the 2004 International Conference on MEMS, NANO and Smart Systems (ICMENS'04)*, vol. 0-7695-2189-4/04, IEEE, 2004.
- [90] J. Darabi, C. Rhodes, CFD modelling of an ion drag micropump, *Sens. Actuators A* 127 (2006) 94–103.
- [91] S. Zeng, C.H. Chen, J.C. Mikkelsen, J.G. Santiago, Fabrication and characterization of electroosmotic micropumps, *Sens. Actuators B: Chem.* 79 (2001) 107–114.
- [92] C.H. Chen, J.G. Santiago, A planar electroosmotic micropump, *J. MEMS* 11 (2002) 672–683.
- [93] L. Chen, H. Wang, J. Ma, C. Wang, Y. Guan, Fabrication and characterization of a multi-stage electroosmotic pump for liquid delivery, *Sens. Actuators B: Chem.* 104 (2005) 117–123.

- [94] Y. Takemori, S. Horiike, T. Nishimoto, H. Nakanishi, T. Yoshida, High pressure electroosmotic pump packed with uniform silica nanospheres, in: Proceedings of the 13th International Conference on Solid State Sensors, Actuators and Microsystems, Seoul, Korea, June 5–9, 2005, vol. 0-7803-8952-2/05/ IEEE, 2005.
- [95] P. Wang, Z. Chen, H.C. Chang, A new electroosmotic pump based on silica monoliths, *Sens. Actuators B: Chem.* 113 (2006) 500–509.
- [96] K.S. Yun, I.J. Cho, J.U. Bu, C.J. Kim, E. Yoon, A surface tension driven micropump for low voltage and low power operations, *J. MEMS* 1.11 (2002) 454–461.
- [97] J.H. Tsai, L. Lin, A thermal bubble actuated micro nozzle-diffuser pump, microelectromechanical systems, in: Proceedings of the 14th IEEE International Conference, 2001, pp. 409–412.
- [98] X. Geng, H. Yuan, H.N. Oguz, A. Prosperetti, Bubble-based micropump for electrically conducting liquids, *J. Micromech. Microeng.* 11 (2001) 270–276.
- [99] J.D. Zahn, A. Deshmukh, A.P. Pisano, D. Liepmann, Continuous on-chip micropumping for microneedle enhanced drug delivery, *Biomed. Microdev.* 6 (2004) 183–190.
- [100] Z. Yin, A. Prosperetti, A microfluidic blinking bubble pump, *J. Micromech. Microeng.* 15 (2005) 643–651.
- [101] J.Y. Jung, H.Y. Kwak, Fabrication and testing of bubble powered micropumps using embedded microheater, *Microfluid Nanofluid* 3 (2007) 161–169.
- [102] R.M. Moroney, et al., Microtransport induced by ultrasonic Lamb waves, *Appl. Phys. Lett.* 59 (1991) 774–776.
- [103] P. Luginbuhl, et al., Microfabricated lamb wave device based on PZT Sol-gel thin film for mechanical transport of solid particles and liquids, *J. Microelectromech. Syst.* 6 (4) (1997) 337–345.
- [104] N.T. Nguyen, A.H. Meng, J. Black, R.M. White, Integrated flow sensor for insitu measurement and control of acoustic streaming in flexural plate wave micropumps, *Sens. Actuators A: Phys.* 79 (2000) 115–121.
- [105] A.H. Meng, N.T. Nguyen, R.M. White, Focused flow micropump using ultrasonic flexural plate waves, *Biomed. Microdev.* 2 (2000) 169–174.
- [106] S. Bohm, B. Timmer, W. Olthuis, P. Bergveld, A closed loop controlled electrochemically actuated microdosing system, *J. Micromech. Microeng.* 10 (2000) 498–504.
- [107] H. Suzuki, R. Yoneyama, A reversible electrochemical nanosyringe pump and some considerations to realize low power consumption, *Sens. Actuators B: Chem.* 86 (2002) 242–250.
- [108] Y. Yoshimi, K. Shinoda, M. Mishima, K. Nakao, K. Munekane, Development of an artificial synapse using an electrochemical micropump, *J. Artif. Organs* 7 (2004) 210–215.
- [109] A. Kabata, H. Suzuki, Microsystem for injection of insulin and monitoring of glucose concentration, in: Proceedings of the 5th International conference on Sensors, Sensors 2005, 2005, pp. 171–174.
- [110] C.S. Effenhauser, H. Harttig, P. Kramer, An evaporation-based disposable micropump concept for continuous monitoring applications, *Biomed. Microdev.* 4 (1) (2002) 27–33.
- [111] V. Namasivayam, R.G. Larson, D.T. Burke, M.A. Burns, Transpiration-based micropump for delivering continuous ultra low flow rates, *J. Micromech. Microeng.* 13 (2003) 261–271.

Biographies

A. Nisar is currently PhD candidate in the department of design and manufacturing engineering at the School of Engineering and Technology, Asian Institute of Technology, AIT, Bangkok, Thailand. His PhD research deals with design and fabrication of MEMS based microfluidic device for biomedical applications. Previously he has done his master of science in advanced manufacturing technology from University of Manchester, United Kingdom in 2002. His post graduate research work has been published in referred journals and conference proceedings. His research interests are finite element modelling of materials, micro/nano electromechanical systems and microfluidics.

Dr. Nitin Afzulpurkar is currently an associate professor and the coordinator of the Mechatronics and the Microelectronics Program, Asian Institute of Technology, Thailand. He obtained PhD from University of Canterbury, New Zealand in mechanical engineering with specialization in Robotics. He has previously worked in India, New Zealand, Japan and Hong Kong. He has authored over seventy five research papers in the field of Robotics, Mechatronics and MEMS. His current research interests are computer vision, MEMS and mechatronic systems. He is a member of IEEE.

Prof. Banchong Mahaisavariya is currently professor of Orthopaedic Surgery, Department of Orthopaedic Surgery, Faculty of Medicine, Siriraj Hospital, Mahidol University, Bangkok, Thailand. He is also deputy dean for Academic affairs, Faculty of Graduate Studies, Mahidol University, Bangkok, Thailand. He obtained his medical degree from Faculty of Medicine, Siriraj Hospital, Mahidol University in 1979. He was observing Fellow at AO Trauma Center at Karlsruhe, Tubingen in 1990. He was also a visiting Fellow in Department of Trauma, University of Innsbruck, Austria in 2002. Previously he has served as Chairman, subcommittee research methodology, Royal College of Orthopaedic Surgeon of Thailand. He is council member, Royal College of Orthopaedic Surgeon of Thailand. He is also editor of the Journal of Thai Orthopaedic Surgeon.

Dr. Adisorn Tuantranont is currently Lab director of Nanoelectronics and MEMS Laboratory, National Electronics and Computer Technology Center (NECTEC), under National Science and Technology Development Agency (NSTDA), Thailand. He is a member of the founding committee of National Nanotechnology Center (NANOTEC), Thailand and Chairman of Thailand's Nanoelectronics Seminar and Training Committee. He has also served as an adjunct senior research scientist and lecturer at Asian Institute of Technology (AIT), Bangkok, Thailand. He obtained PhD in 2001 from University of Colorado at Boulder, Colorado, USA, in electrical engineering with specialization in Optical MEMS and Laser and Optics System. His current research interests are optical MEMS, Microfluidic Lab-on-a-chip and optoelectronics packaging. He has over 100 papers published in refereed journals and conference proceedings. He received Thailand Young Technologist Award in 2004.